Habitability on local, Galactic and cosmological scales

Luigi Secco[1] • **Marco Fecchio[1]** •
Francesco Marzari[1]

Abstract The aim of this paper is to underline conditions necessary for the emergence and development of life. They are placed at local planetary scale, at Galactic scale and within the cosmological evolution, as pointed out by the Anthropic Cosmological Principle. We will consider the circumstellar habitable zone (CHZ) for planetary systems and a Galactic Habitable Zone (GHZ) including also a set of strong cosmological constraints to allow life (cosmological habitability (COSH)). Some requirements are specific of a single scale and its related physical phenomena, while others are due to the conspired effects occurring at more than one scale. The scenario emerging from this analysis is that all the habitability conditions here detailed must at least be met. Then life asks something which may appear as "a monstrous sequence of accidents" as Hoyle (1959) thought, or as providential collaborations leading to realize how finely tuned is the architecture within which Life, as precious stone, is embedded.

1 Introduction

The first step is to specify to what life we refer. This leads to the essential requests that must be fulfilled to allow the development of this kind of life (sect.2) and to which astrophysical scales they mainly are related (sect.3). In sect.4 we point out how in the Solar system, among ten planets and hundreds of satellites, life in complex form appears only on Earth, proving to be peculiar without being probably exclusive. Some of the many constraints on arising and developing of it may be detectable studying our site. The Climatic Astronomical Theory is introduced in sect.5 in order to define the circumsolar habitable zone (HZ) (sect.6) while the translation from Solar to extra-Solar systems leads to a generalized circumstellar habitable zone (CHZ) defined in sect.7 with some exemplifications to the Gliese-667C and the TRAPPIST-1 systems; some general remarks follow (sect.8). A first conclusion related to CHZ is done moving toward GHZ and COSH (sect.9). The conditions for the development of life are indeed only partially connected to the local scale in which a planet is located. A strong interplay between different scales exists and each single contribution to life from individual scales is difficult to be isolated. However we will limit ourselves to a first order approach in which the analyzed necessary ingredients for life are first of all linked to a given main scale, taking the more complex connections with the others as considerations of second order.

In sect.10 we will introduce the Galactic Habitable Zone (GHZ) to which mostly leads the following requests: i) the metal amount necessary to form a planet like Earth, ii) quantify the threats of supernovae explosions. The main contributions from different authors on the GHZ limits are also analyzed. Then we consider the role of possible comet injections from Oort's Cloud (or analogs) due to tidal effects coming from the main dynamical Galaxy components (sect.11). In sect.12 we add a new constraint to GHZ due to the possibility of a comet flux with relevant consequence for life. That is bound to the location of planetary system on Galactic plane. Further a probable Solar path through the Galaxy has to be considered owing to the Sun's over-metallicity. In this way we will be forced to move to the wider history of Galaxy formation and to its chemical-dynamical evolution. Some paths have been simulated (Kaib et al., 2011) and overlapped to GHZ (sect.13). Then the horizon gets larger to the cosmology where

Luigi Secco

Marco Fecchio

Francesco Marzari

[1]Department of Physics & Astronomy, Padova University

many fine tunings exist in the connection between some factors constraining the main features and evolution of Universe and life. The set of these fine tuned cosmological constraints define, in our view, the cosmological habitability (COSH) (sect.14). Conclusions are given in sect.15.

2 What kind of life?

What kind of life are we referring to? We focus on the typical life on Earth, the only one we know so far, therefore we consider environments suitable to aerobic complex life based on oxigen and carbon excluding the wide spectrum of life-forms limited at microorganism level. In addition, all organisms we are familiar with require liquid water during at least part of their life cycle. Here below we summarize the essential requests for this kind of life in order of decreasing priority (Dallaporta & Secco 1993) and putting in brackets the scales to which they mainly refer (see, sect.3):

- α) the presence of bricks, it means the chemical elements which are basilar in order to form organic compounds. As mentioned in Barrow and Tipler (1986), the biochemist Lehninger (1975) divided the chemical elements important for life into three main classes. In class one there are the essential elements which are present (for one per cent or more) in all living organisms (with the exception of sulphur). They are oxygen, carbon, nitrogen, hydrogen, phosphorus, and sulphur. In class two it appears the monoatomic ions, such as N_a^+ and K^+, in class three the trace elements: iron, copper and so one.

  In COSH, we will take into account how special is the tuning of coupling constants in producing primordial helium at the beginning of Universe and how carbon and oxygen burnings occur later inside the first star generation. In addition, in Appendix we will outline the main nuclear reactions able to produce nitrogen and phosphorous inside stars (COSH).

- β) A sufficiently long time as the terrestrial experience teaches us. Indeed the earliest micro-fossil evidence for life is about 3.5 billion years old, that is at least $\simeq 1 \cdot 10^9 yr$ after the formation of the planet. They are unicellular and prokaryote organisms from some of the oldest rocks on the planet, similar to bacteria and to blue green algae. Moreover to reach complex, pluricellular eukaryotic forms of life it is necessary to add another $\simeq 2.7 \cdot 10^9 yr$ (Fig.1)(Simpson, 1986, pg.71; Curtis & Barnes, 1991; for an updated and detailed timetable of life developing in: Eons, Eras, Periods and Ages, see, Knoll & Nowak, 2017) (GHZ, COSH).

The following elements are essential in the nutrition of one of more species, but not all are essential for every species	
Class one elements: The elements of organic matter	Class three elements: Trace elements
O	Mn
C	Fe
N	Co
H	Cu
P	Zn
S	B
	Al
Class two elements: Monoatomic ions	V
Na^+	Mo
K^+	I
Mg^{2+}	Si
Ca^{2+}	Sn
Cl^-	Ni
	Cr
	F
	Se

Fig. 1 The elements used in living organisms, see text, Barrow and Tipler (1986), pg.553.

- γ) Planetary conditions suitable to harbour life. This means orbital stability leading to steady atmospheric temperature and pressure (organic compounds have to find not only the possibility to form but also to be stable). Their values must also be compatible with the presence of liquid water on the surface (CHZ).
- δ) In addition, the environment has to be suitable to form long molecular biological chains (CHZ and GHZ).

Human Life might request more stringent constraints.

3 The different scales

Each of the essential requests: α), β), γ), δ) are mainly linked to the physical phenomena occurring at one of the three scales of habitability considered:

- Local or planetary: it defines a circumstellar habitable zone (CHZ) on the basis of the *greenhouse effect* and the presence of liquid water.
- Galactic: it deals with the metal amount needed to obtain a terrestrial planet, the effects of supernovae explosions, the Galactic tide on comets and the necessary time for developing complex life. These constraints leads to the definition of Galactic habitable zone (GHZ).
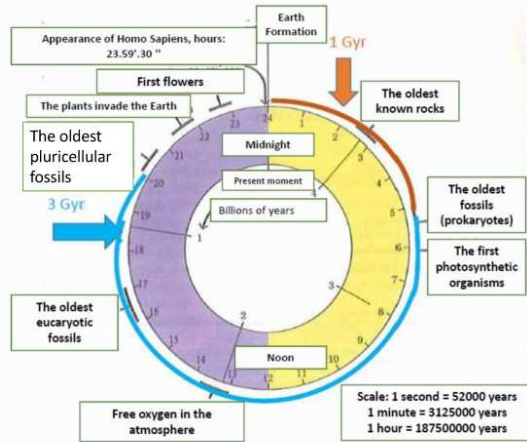
Fig. 2 The biological time clock: the age of Solar system (4.5 Gyr) is divided into 24 hours, 60 minutes and seconds. The correspondence is shown in the legend. After Earth formation primordial unicellular and prokaryote organisms needed at least $\simeq 1 \cdot 10^9 yr$ to appear (before six a.m.; red line and arrow). To reach complex pluricellular eukaryotic forms of life we need to add again about 3 Gyr (around 8 p.m.; blue line and arrow) (adapted from:*Curtis & Barnes, 1991*).

- Cosmological: it involves the relationship between life and cosmological evolution and it outlines the cosmological habitability (COSH).

It frequently happens that constraints from one scale correlate to those of another one making it difficult to disintangle the individual contribution. In sect.2, we have put in brackets some indications to drive the reader through the items.

PARAMETER	VENUS	MARS	REFERENCE
Mean heliocentric distance (AU)	0.723	1.524	1
Surface temperature (K)	733	215	2, 3
Surface pressure (bar)	92	0.0056	2, 3
Bond Albedo	0.75	0.16	1, 2, 4, 5
Scale height of the Atmosphere (km)	15	11	8
Exobase temperature (K)	275, 1020	350	2
Satellites	ABSENT	PHOBOS AND DEIMOS, THEY ARE NOT SUFFICIENT TO STABILIZE THE OBLIQUITY OF THE PLANET	7
Magnet c Field	WEAK	WEAK	8
Escape Velocity (km/h)	10.4	5.04	8
Water at Liquid State	ABSENT	ABSENT	8

Fig. 3 Collections of different characteristics related to our neighbors: Mars and Venus (references: 1, Yoder (1995); 2, Chamberlain & Hunten (1987); 3, Clarke et al. (1992); 4, Veverka et al. (1988); 5, Moroz (1983); 6, Stern and Yelle (1999), in De Pater e Lissauer (2001); 7, Tomasella et al. (1996); 8, Marzari & Vanzani (2013)).

4 The Earth peculiarity

We collect here some features that allowed the Earth to reach suitable conditions for life and compare them with those of our neighbooring planets (Fig.3).
The aim doesn't go in the direction to exclude other possible life like that on the Earth, but realistically to analyze the necessary constraints to allow it. Peculiarity indeed doesn't mean exclusivity. According to the Weak Anthropic Principle (see, sect.15) the fine tuned conditions of the Universe are in fact to obtain life, as the only one we know, but spread in the whole Universe.

- Its revolution around the Sun is placed at a distance (1 AU) that permits the presence of water in a liquid, solid and gaseous state on its surface;
- its atmosphere is mainly composed by nitrogen and oxygen;
- the intensity of its magnetic field (0.3-0.4 G) is the highest within the Terrestrial Planets so that it can act as a shield against cosmic rays and solar wind;
- among the Terrestrial Planets, Earth is the most massive and the escape velocity turns out to be very high (11.2 km/sec). The consequence is a stable atmosphere with a reduced thermal loss of atmospheric components.
- Its only satellite, the Moon, is massive ($\simeq 1/80 \, M_\oplus$; the highest ratio in the Ss) and close enough ($\simeq 30 \, d_\oplus$) to stabilize the Earth obliquity allowing a regular succession of seasons on a very long time-scale (see, sect.5.2 for a wider discussion).
- The existence of Earth's plate tectonics which has a crucial role in the geochemical carbonate - silicate cycle as discussed in the next sect. 6.1.1. From the preliminary results of Noack & Breuer (2011) it seems that propensity of plate tectonics may occur more seldom than previously thought with a peak between one and five Earth masses. For Mars, in comparison, there are a number of lines of circumstantial evidence to suggest that it did in the past have some form of surface tectonics or tectonic episodes but the problem remains completely unresolved (Zhang & O'Neil, 2016). Moreover, about the volcanism which is essential part of geochemical cycle, thermal evolution models of Mars suggest that its volcanism should have stopped at least some hundred million years ago (Hauck and Phillips, 2002; Breuer and Spohn, 2003), although it is possible that Mars is not yet volcanically extinct as claimed by Hauber et al., 2011.

In Fig.4 Earth, Mars and Venus' temperature gradients are also compared. They become relevant in determining the greehouse effect (e.g. the tendency of water vapor to escape from the Earth is minimal while this is not the case for the early Venus (Kasting et al., 1988)).
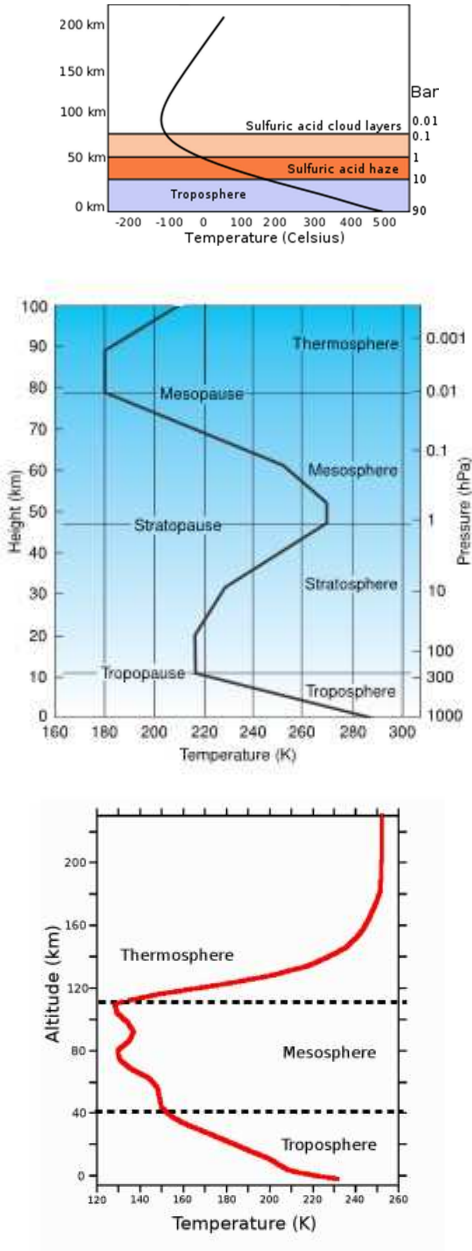
Fig. 5 Evolution of Earth's obliquity, θ, for the real Earth-Moon system (continuous line) and in a test case where Moon's distance from Earh is increased from 60.3 to about 66.5 terrestrial radii (dotted line) (Tomasella et al., 1996).

Fig. 4 From top to bottom: Venus, Earth and Mars' temperature gradients. Credits: Palen et al. (2011); Wallace & Hobbs, (2006) ; González-Galindo et al. (2008), respectively.
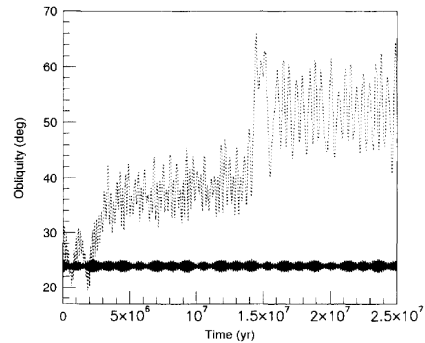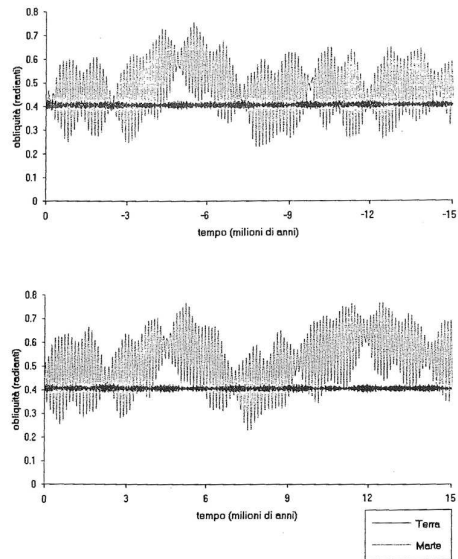
Fig. 6 Comparison between the variations of obliquity θ of Mars in the Mars-Phobos-Deimos system (dotted line) vs that of Earth in the Earth-Moon system (continuous line) for 15 million years before (upper) and after present (down) (simulations by Tomasella, 1992). Mars maximum oscillations are of $\pm 15.4^{o}$ around the mean value of 23.4^{o}.

5 Relationship between climatic history and dynamics

Since the beginning of 1900, various models relating the climatic history of a planet with its dynamical evolution within Ss have been formulated leading to the so called Climatic Astronomical Theory (e.g., see, Ward, 1974). Ad example, Earth's mean temperature depends not only on the Earth-Sun distance which determines the Solar flux on the planet, but it is also subordinate (as we will see) to its dynamics and to the climate model for its atmosphere (sect.6) (Kasting et al., 1988; Kasting et al., 1993).

5.1 Orbital elements

Usually, the main orbital elements relevant in the determination of the planet's temperature are the eccentricity e, longitude of perihelion ϖ and the semimajor axis a. In addition, also the obliquity θ has a relevant role. The average *insolation* during a periodic revolution, can be estimated at the planet's pole (Ward, 1974) as:

$$\langle I \rangle = S\ sin\theta/\pi\ (1 - e^2)^{-1/2} \tag{1}$$

where S is the Solar constant, S_o, scaled at the planet's distance in AU.

5.2 On Earth's obliquity

Due to the fast rotation around its axis, the Earth shape becomes spheroidal with an equatorial semimajor axis larger than the semiminor one of about 21 km. This causes a precession of its rotational axis due to the Luni-Solar effect with a period equal to about $T_{p\oplus} \simeq 26,000\ yrs$. It is the fastest precession rate in the Ss (e.g., for Mars, $T_{pM} \simeq 175,000\ yrs$), placing at present the Earth far from resonances between its precession motion and any fundamental frequency of the secular motion of the Ss which might cause a chaotic evolution of the obliquity of the planet (Laskar & Robutel, 1993; Tomasella et al., 1996; Neron de Surgy & Laskar, 1997). The occurrence of these resonances depend on the architecture of the planetary system which sets the fundamental frequencies of its secular evolution and the precession rate of the planet spin axis which may be determined by the presence of a satellite. In the case of the Earth, the Moon may lead in the future the Earth into a chaotic state when the tidal interaction between the two bodies will have moved the Moon to 66.5 Earth's radii (it is currently at 60). This is shown in Fig.5 illustrating the evolution of the Earth obliquity

as the Moon moves from its current distance of 60.3 terrestrial radii (continuous line) to 66.5 (dotted line) (Tomasella et al., 1996). This behavior is compared to that of Mars (Fig.6) where its obliquity cannot avoid, due to the small masses of Phobos and Deimos, variations of its rotazional axis up to $\pm 15.4^o$ around a mean value of 23.4^o. This behavior leads to an important requirement for a planet to be habitable i.e. that its precession rate be far from any fundamental frequency of the system whose values are determined by the mass and semimajor axes of all planets in the system.

5.3 The greenhouse effect

The temperature of a planet surface is strongly depending on *the greenhouse effect* due to the planet atmosphere. To roughly quantify its relevance, let us remember the approximate results for Earth and Mars, collected in Fig.7, obtained by a simplified atmospheric model (Ortolani, 2012; Davolio, 2012). The solar flux incident at the top of the atmosphere is equal to the present solar constant at Earth's orbit, $S_o = 1360\ W\ m^{-2}$. The radiative balance between the flux coming in from Sun, S, and that emitted from planet surface of radius R, as a black-body with effective temperature T_e, without atmosphere, reads as:

$$S = (1 - A)\frac{S_o}{4} = \sigma T_e^4 \tag{2}$$

σ being the Stefan-Boltzmann constant, A the planetary (Bond) albedo. If T_s is the surface temperature when atmosphere is present and T_A the temperature of a single *greenhouse gas layer*, the inclusion of its contribution, transforms (2) into:

$$(1 - A)\frac{S_o}{4} + \epsilon\sigma T_A^4 = \sigma T_s^4 \tag{3}$$

because the atmosphere radiates equally outwards and inwards. The relationship between T_e and T_s becomes:

$$\frac{T_s^4}{T_e^4} = \frac{1}{1 - \epsilon/2} \tag{4}$$

Where ϵ is the *emissivity* of the atmosphere.

5.3.1 To quantify greenhouse effect

The present Earth's atmosphere is done, as percentage by weight, of nitrogen, 78%, of oxygen, 21%, of argon 1%, of carbon dioxide, 0.03%.
The fraction of Solar flux reflected by the high part

of the atmosphere, for Earth (in the visible range) is: $A \sim 0.3$ (Pallé et al. 2016). Many factors are involved in determining both *albedo* and the emissivity ϵ of an atmosphere:

- the amount of lands;
- the amount of condensed volatile substances (extension of ice caps, of liquid fraction and cloud conformation).

For the Earth, the UV radiation, in the range $200 \div 300nm$, is absorbed by the ozone in the *stratosphere* while the IR component is absorbed by the *troposphere* which in turn diffuses it inside thanks to the presence of water vapor and CO_2. The amounts of both these components determine the *greenhouse effect* (Fig.8).

6 Circumstellar Habitable Zone for Solar system (HZ)

6.1 Standard climate Model

In order to estimate the width of the HZ around stars similar to our own Sun we introduce the standard climate model for the Earth and Terrestrial Planets in general, as proposed by Kasting et al. (1988), Kasting et al.(1993). In this model the atmospheres are made of $CO_2/H_2O/N_2$.

The vapor pressure of water at the surface is a function of surface temperature. In most of the calculations of this 1-D model, N_2 is at 1 bar of pressure while CO_2 has a variable partial pressure and H_2O and CO_2 clouds are not included explicitely.

6.1.1 The role of carbon dioxide

Due to its four electrons in the L shell carbon form a double bond with oxigen in CO_2. Since each oxygen atom has a valence of two, the double bond completes the L shell of each oxygen atom, and carbon dioxide molecule has very little remaining affinity for itself.

PLANET	A	ε	Te(K)	Ts(K)
EARTH	0.30	0.6	255	288
MARS	0.24	0.09	213	218

Fig. 7 Comparison of global *albedo* A (in visible range), emissivity ϵ, effective temperatures T_e and surface temperatures T_s, between Mars and Earth (Eqs. 2, 3, 4) for a simplified atmospheric model (see, text) (Ortolani, 2012; Pallé et al. 2016).

This means that carbon dioxide is a gas at ordinary temperatures.[1]

CO_2 and its evolution is governed by carbonate-silicate geochemical cycle. Following Kasting et al. (1988) and Kasting (2001), we may summarize it as follows: CO_2 is emitted from volcanoes and from atmosphere it dissolves in rainwater which erodes rocks that contain calcium-silicate minerals (C_aSiO_3). In the chemical process calcium and bicarbonate ions (Ca^{++} and HCO_3^-) are released into the groundwater and ultimately transported to the ocean. In the sea, plankton and other organisms incorporate them. When the organisms die, they will form the carbonate sediments at the bottom of the ocean. When seafloor is subducted as a result of plate tectonics activity, calcium carbonate (C_aCO_3) subjected to rising temperature and pressure reacts with silica re-forming silicate rocks and releasing gaseous carbon dioxide by , e.g., volcanic eruptions. As highlighted by Kasting et al. (1988) that is a feedback system owing to the Earth's temperature has always remained within reasonable limits even though for stellar evolution Sun changed its luminosity of about $(25 \div 30)\%$ during the 4.5 billion years from the formation of solar system. *Thus the carbonate-silicate cycle acts as a planetary thermostat that regulates mean surface temperatures* (Ramirez, 2018). Without it the Earth's atmosphere would be only marginally stable, which means it could be destabilized by relatively small perturbations. That indeed occurs in the Hart's computer simulations (Hart, 1978.) According to them, as the free oxygen concentration gradually rose from zero in the beginning to the current level due to phothosynthesis of green plants the greenhouse effect faded away with the effect that the temperature decreased drastically (Barrow & Tipler, 1986, Chapt.8).

6.1.2 The effective Solar flux

The radiative model assumes a fixed surface temperature (which of course is not determined only by Solar flux but by all climatic factors entering the greenhouse effect) and the model is used to calculate the required net incident Solar flux, F_S, and the net outgoing infrared flux, F_{IR}, at the top of the atmosphere.

The *effective Solar flux*, S_{eff}, is introduced as:

$$S_{eff} = S/S_o = \frac{F_{IR}}{F_S} \tag{5}$$

---

[1]That doesn't occur,e.g., for silicon dioxide which is a solid, even though silicon is very similar to carbon and has the same valence of four.

It is noteworthy that (5) is not a simply definition but the equality between the two last terms corresponds to two energy balances. The requirement is indeed the following: without atmosphere, but in the presence of *albedo*, the ratio S to S_o is the fraction of incoming flux on the planet, needed to maintain a given effective surface temperature, T_e. It corresponds to the energy balance of Eq.(2), it means a given ratio is requested between the emitted flux from Earth's surface (or planet's surface) and the incident one S_o. This ratio must be equal also, when the atmosphere is present, to the ratio between the net outgoing IR flux from atmosphere and the net incident solar flux F_S needed to obtain a given surface temperature T_s (energy balances of Eq. (3)), both evaluated at the top of atmosphere (see, also the qualitative picture of Fig.8) (Kasting et al., 1993, Kopparapu et al. 2013).

The planetary global *albedo* is then obtained from the following expression[2] :

$$A = 1 - \frac{4F_S}{S_o} \qquad (6)$$

Calculations based on this model were performed considering surface temperature, T_s, incrementaly growing from 220 K up to 2200 K (see, Kopparapu et al., (2013) which updated the Kasting et al. (1993) model).

From the energy balance (5) it immediately follows that: if the planet moves from 1 AU to d AU, S and S_{eff}, scale according to:

$$S \Rightarrow S_{eff} \sim 1/d^2 \qquad (7)$$

S_o remaining fixed at Earth's orbit.

Moreover, if the luminosity of the central star in the planetary system changes, the following scaling law holds:

$$d = 1AU \left(\frac{L/L_\odot}{S_{eff}} \right)^{0.5} \qquad (8)$$

6.1.3 Inner edge (IHZ)

The dependence of various physical quantities on surface temperature for the inner edge of HZ derived from the standard model are shown in Fig. 9, 10, 11 (Kopparapu et al., 2013). Two limits for the inner edge can be calculated:

- the first one is the *moist-greenhouse* or *water-loss* limit (Fig.11). It occours at a surface temperature of 340 K ($\sim 67^oC$) when $S_{eff} = 1.015$.Under these conditions the water vapor content in the stratosphere increases dramatically, by more than an order of magnitude. The orbital distance corresponding to the cloud-free water-loss limit is $d = 1/S_{eff}^{0.5} = 0.99AU$ for an Earth-like planet orbiting the Sun. That is considered a *pessimistic inner edge distance.*
- The second one is the *runaway greenhouse* limit where the oceans evaporate entirely corresponding to $d = 0.97AU$. The surface temperature at which it occours is about 1800 K ($\sim 527^oC$). This inner edge located closer to the star has to be considered a *more optimistic inner edge.*

When the *moist-greenhouse* limit is considered as inner bord, the criterium of *water-loss* has to be taken into account, via *photolysis* process in which the atmospheric H_2O vapor molecules dissociate into H^+ and OH^- ions, and the consequence of hydrogen escape (Kasting et al.,1993). The possible feedback of clouds is ignored. In the model of Kasting et al. (1993), the background atmosphere consists of 1 bar of N_2 and 300 parts per million by volume of CO_2, with no oxygen or ozone. In the model of Kopparapu et al. (2013) the background gas is instead made of 4 bar of N_2 and the total surface pressure is 6.5 bar.

6.1.4 Outer edge (OHZ)

To compute the outer edge, the Earth-like surface temperature was fixed at 273 K and the atmosphere was assumed to consist of 1 bar of N_2 while the CO_2 partial pressure was varied from 1 to 35 bar (the saturation vapor pressure for CO_2 at that temperature) (Kopparapu et al., 2013). The working hypothesis is that atmospheric CO_2 would accumulate as the surface temperature decreases owing to the negative feedback provided by carbonate-silicate geochemical cycle.

To understand the existence of a *maximum limit* for the greenhouse, we have to calculate the flux ratio (S_{eff}) required to mantain a global mean surface temperature of 273 K when CO_2 condensation, due to the increasing distance from Sun, occurs.The incident F_S decreases monotonically with increasing CO_2 partial pressure (Fig.12) as a result of enhanced Rayleigh scattering. Correspondingly the planetary albedo increases (Fig.13). F_{IR} decreases initially as CO_2 partial pressure grows. This is an indication of the *greenhouse effect* of CO_2 (Fig.12). At about 10 bar, it asimptotically approaches a constant value as the atmosphere becomes optically thick at all IR wavelengths. So a minimum in S_{eff} (Fig.14) occurs at CO_2 partial pressure of ~ 8 *bar* corresponding to a maximum distance
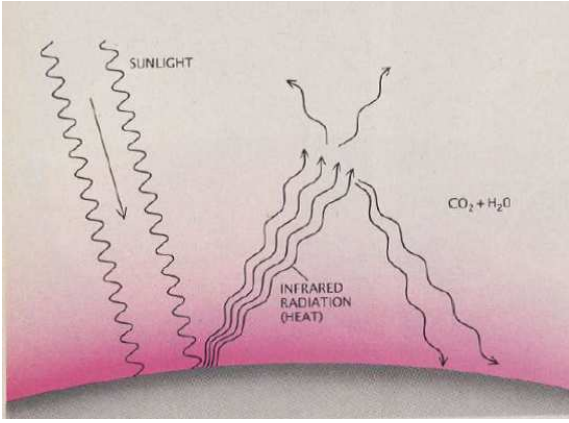
Fig. 8 Qualitative picture to understand the energy balance (5) when the atmosphere produces *greenhouse effect*. Carbon dioxide and water vapor intercept the infrared rays (heat) that planet radiates into space and reradiate much of this energy toward the surface. Only part of this infrared radiation escapes from the top of the atmosphere. (Kasting et al., 1988).

$d = 1.67 AU$ which defines the *maximum greenhouse* limit for the outer edge. It is very interesting to note that the end of the greenhouse effect is essentially due to conspiracy of two effects together: the decreasing of the F_S owing to the increasing distance from Sun and the enhancement of Rayleigh scattering. At the same time, the F_{IR} decreases while the reflecting power increases, as shown by the albedo trend (Fig.13). All that occurs in agreement with Kirchhoff's law: the emitted flux decreases as the absorbed one. Beyond this distance, S_{eff} increases and the surface temperature of $0^o C$ is no more guaranteed by greenhouse effect.

6.2 Venus and Mars as empirical optimistic limits

We may notice that Venus, which is located at a distance $d = 0.72\ AU$, is too close to the Sun since the inner edge of the HZ is equal to 0.97 AU. However, Venus had surface features due to liquid water, which are absent for at least 1 Gyr. Then taking into account that the Sun at that time had about $\sim 92\%$ of the present-day luminosity, Kasting et al. (1993) and Kopparapu et al. (2013) conclude that the IHZ might have been as low as 0.75 AU (recent Venus) suggesting that Venus was on the brink of a runaway greenhouse effect causing the disappear of liquid water. As for the inner edge model, a more optimistic empirical limit on the OHZ (Outer HZ) may be derived from the observation that the early Mars was warm enough for liquid water to flow on its surface when it was old of 3.8 Gyr. Even though the problem is still an open issue, taking

into account that the Solar luminosity at that time was $\sim 75\%$ of the present one, scaling the flux received by present Mars of that of Earth's to the early Mars, Kasting et al. (1993) and Kopparapu et al. (2013) move the Mars distance from 1.52 AU to 1.77 AU for the early Mars.

6.3 Conservative and Optimistic HZ

Following Kane et al. (2016), we summarize the limits of HZ obtained using the 1-D model considered:

- IHZ: *moist and runaway greenhouse*, $0.99 \div 0.97\ AU$; (*recent Venus*: 0.75 AU),
- OHZ: *maximum greenhouse*, 1.67 AU; (*early Mars*: 1.77 AU).

After the updated absorption coefficients for CO_2 and H_2O (Kopparapu et al., 2013, 2014) the two IHZ have coalesced to 0.99 AU. So the *conservative theoretical HZ limits* and the corresponding values of the effective solar flux are, respectively:

$$d = (0.99\ (0.95) - 1.7)\ AU$$

$$S_{eff(Sun)} = (1.02\ (1.11) - 0.36)$$

whereas the *optimistic empirical HZ limits* and the corresponding values of the effective solar flux are, respectively:

$$d = (0.75 - 1.8)\ AU.$$

$$S_{eff(Sun)} = (1.78 - 0.32)$$

To be noted that a better estimate for a theoretical IHZ is 0.95 AU (Leconte et al. (2013) by 3-D models, sect. 6.3.2).

6.3.1 Effect of clouds

The HZ boundaries is strongly influenced by the presence of clouds (H_2O and CO_2 clouds), even though quantitative statements are difficult. Their either warming or cooling effect depend on many parameters, e.g., their height, optical depth, particle size, and, most importantly, fractional cloud coverage. Calculations suggeste that CO_2 clouds should generally warm the climate rather than cool (Mischna et al., 2000). But on this topic the research is still in progress using 3-D models.

An additional atmospheric effect may be related to the presence of thick hazes like that observed on Titan. On one side they may cool the planet surface by about 20 K extending the inner edge of the HZ but they may also grant UV shielding enhancing planetary habitability (Arney et al., 2016).
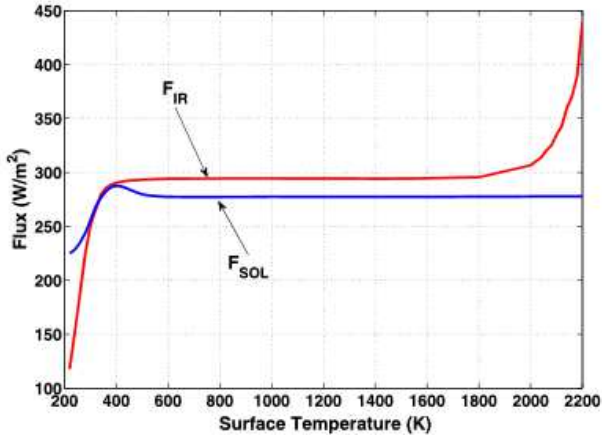
Fig. 9 Trends of fluxes (F_{IR} and $F_{SOL} = F_S$) as function of surface temperature for the standard inner edge model (Kopparapu et al., 2013).

6.3.2 Extension of the HZ

A significant broadening of the HZ, in particular the outer edge, can occur adding additional greenhouse gases. Specifically if volcanism on terrestrial planets can maintain large amounts of molecular hydrogen, a very light greenhouse gas (Ramirez & Kaltenegger, 2017). Hydrogen retention might be more efficient on super-Earths where the escape rates are lower due to stronger gravity and the interior heat lasts longer favouring vulcanism and H_2 outgassing. This mechanism, if active, may extend the outer edge of the classical HZ by as much as 60% (Ramirez & Kaltenegger, 2017).

As climate models improve also the theoretical HZ limits evolve. 3-D climate models may include, e.g., factors such as variations in relative humidity and clouds which are impossible to estimate accurately in 1-D calculations. So by a 3-D study, Leconte et al. (2013) move the IHZ to at least 0.95 AU. Also the inner edge of the HZ has been considered with 3-D climate model, for dry planets, sometimes called "Dune" planets. A (low-obliquity) planet of this kind would have water-rich oases near its poles. For such a planet with a Sun-like star, the IHZ could be as close as 0.77 AU, about the empirical *recent Venus* limit.

The inner edge of the HZ has been pushed closer to the host star (until about 0.38 AU around a Solar-like star) if the *greenhouse effect* is reduced (low relative humidity) and the surface *albedo* is increased (Zsom et al., 2013). However this result has been criticized by Kasting et al. (2014). In conclusion, because it may take time for different models to reach consensus, we may refer to both conservative and optimistic estimates of the HZ from the 1-D model of Kopparapu et al. (2014)
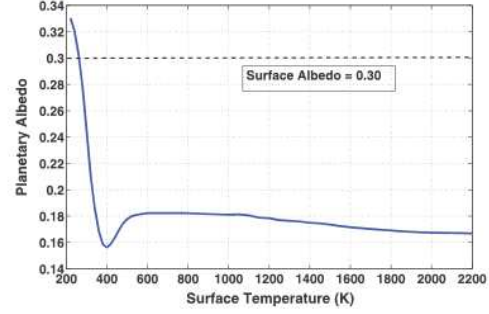

Fig. 10 As in Fig.9, for planetary *albedo* according to (6). The dashed line shows the assumed surface global *albedo* (Kasting et al., 1993; Kopparapu et al., 2013c, Erratum).
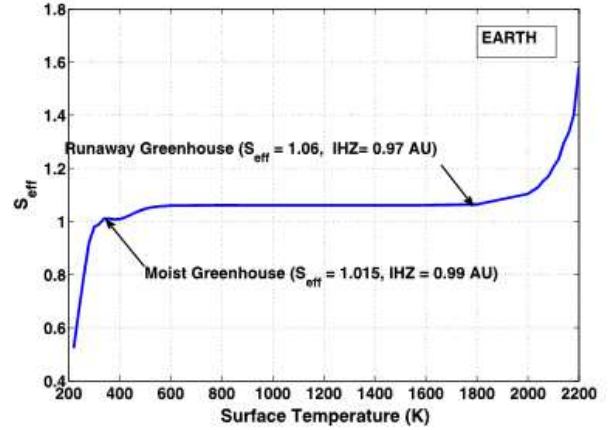

Fig. 11 As in Fig.9, for effective solar flux, S_{eff} with the two relevant inner limits, *water-loss* (at a surface temperature of 340 K ($\sim 67^{o}C$)) and *runaway greehouse* (at about 1800 K ($\sim 527^{o}C$)). (Kopparapu et al., 2013).

encompassing the limits from 3-D models (Kane et al., 2016, Fig.1).

7 Circumstellar Habitable Zone (CHZ) for extra-Solar systems

7.1 The method's generalization

Kopparapu et al. (2013) update the database used by Kasting et al. (1993) to build up their climatic model in the case in which at the center of the extra-Solar system there is a main-sequence star of spectral type F, G, K, M. The stellar effective temperature is in the range $2600\ K \leq T_{eff} \leq 7200\ K$. Classical HZ boundaries have been derived using the key Eq.8, and the following relationship between HZ stellar fluxes (S_{eff}) reaching the top of atmosphere of an Earth-like planet and the stellar effective temperatures (T_{eff}) in the range
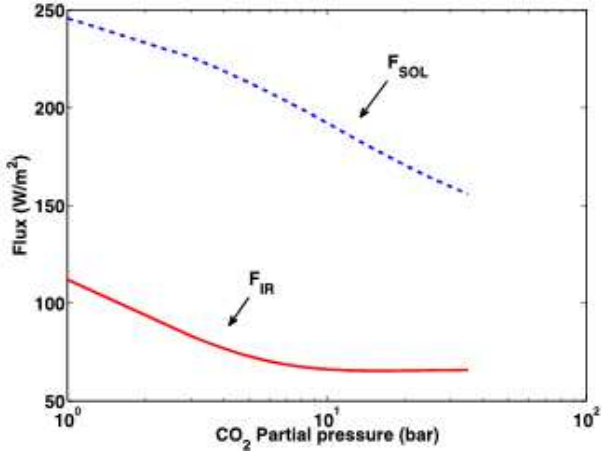
Fig. 12 Outer edge of HZ from climate model. Trends of Fluxes, like Fig.9, as function of CO_2 partial pressure. The mean surface temperature is fixed at 273 K (Kopparapu et al., 2013).
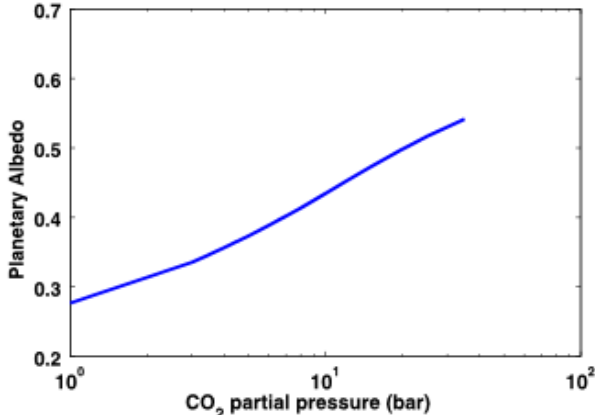

Fig. 13 As in Fig.12, for planetary *albedo* (Kopparapu et al., 2013).

considered:

$$S_{eff} = S_{eff\odot} + aT_* + bT_*^2 + cT_*^3 + dT_*^4 \qquad (9)$$

where $T_* = T_{eff} - 5780\ K$ and $S_{eff\odot}$ is the the S_{eff} value for a given HZ limit in our Solar system. The trends of S_{eff} as function of surface temperature (for the inner edge) and of partial CO_2 pressure (for the outer one) are similar to those of the Sun for each T_{eff} in the range $2600 \div 7200$ (Fig.15 vs. Figs.11,14). Recently the temperature range has been expanded to $10,000\ K$ including then A-stars (Ramirez & Kaltenegger, 2018). The quantities (a,b,c,d) are constant coefficients listed in Table 1 of Ramirez (2018). This allows to define the Habitable Zone, with both limits *conservative* and *empirical* in analogy with Solar system
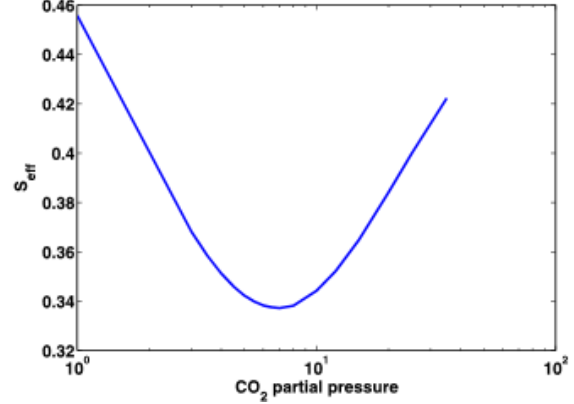

Fig. 14 As in Fig.12, for S_{eff}. Its minimum defines the *maximum greenhouse limit* (Kopparapu et al., 2013).

(sect.6.3), for a general planetary system around a main sequence star as plotted in Fig.16. Some specific exemplifications are shown for Gliese-667C and TRAPPIST-1 systems.

7.2 Application to the Gliese-667C and to the TRAPPIST-1 systems

The result for the optimistic HZ is shown in the case of extra-Solar system with an M star (like Gliese-667C) at the center (artistic picture of Fig.17). The characteristics of corresponding planets are listed in Anglada-Escudé et al., 2013.

The TRAPPIST-1 is an ultracool M dwarf with effective temperature of less than 2,700 K (Gillon et al., 2016). The seven planets of the system orbit the star with semi-major axes < 0.1 AU and orbital periods of a few Earth days (Barr et al., 2018). Due to the star's low luminosity each planet has a moderate temperature, ranging from $\sim 160\ K$ to 400 K. These low temperatures suggest that some might have solid surfaces composed of H_2O ice and/or rock. Due to their non-zero orbital eccentricities tidal forces vary with time resulting in heating of their interiors by tidal dissipation. Tidal heating is an important energy source also in Ss for the satellites of the outer planets (e.g. for moons of Jupiter and Saturn).

Trappist-1d and Trappist-1e might potentially be habitable (Fig.18).Trappist-1d appears also in Fig.16 within the *empirical limits* whereas Trappist-1h lies on the border of the same HZ. According to the models performed by Barr et al. (2018), planet d could have a liquid water ocean at the surface and it might avoid the *runaway greenhouse* state if its albedo is ≥ 0.3. It seems also that the e planet could harbor a thick ice mantle with likely liquid ocean underneath. To rule out a water-free structure, one needs to determine better
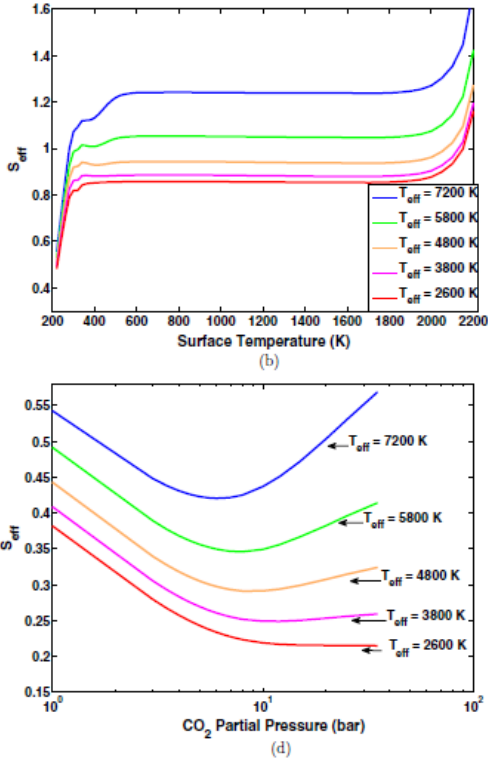
(b)

(d)

Fig. 15 Trends of S_{eff} as function of surface temperature (for the inner edge, (b)) and of partial CO_2 pressure (for the outer one, (d)) for each T_{eff} of the main- sequence stars hosting extra-Solar planetary systems, in the range $2600 \div 7200$.
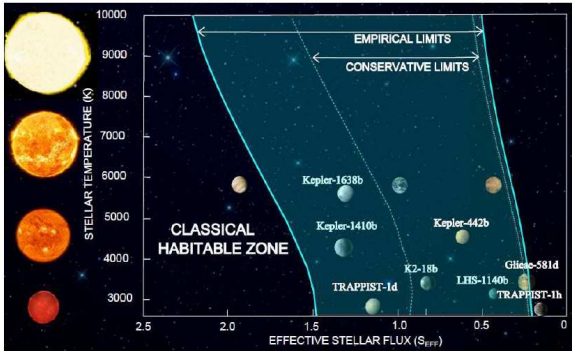

Fig. 16 Habitable zone with *conservative* and *empirical* limits in analogy with Solar system (sect.6.3), for a general planetary system around a main sequence star from 2600 to 10,000 K. Planets of TRAPPIST-1 systems, discussed in the text, are also shown (Ramirez, 2018).

the mass, to within $\sim 0.5 M_\oplus$. However, observations of TRAPPIST-1 showed frequent flares which constitute a serious threat for planetary atmospheres. Strong magnetic fields would be required to protect life from high energy radiation. Also the likelihood function for
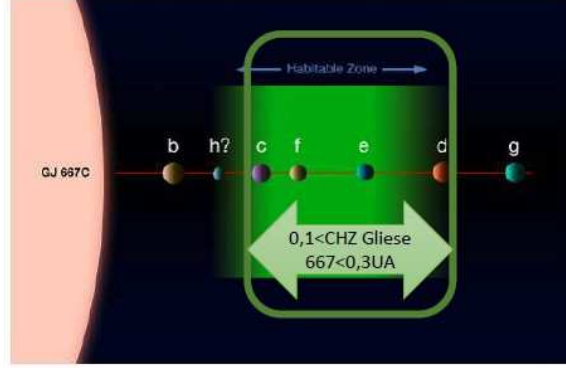

Fig. 17 Artistic picture of HZ in the Gliese-667C system (credit: ESO, adapted by Fecchio, 2016). The two planets at the limit of HZ correspond to about the optimistic limits which, in the Solar system, are given by *recent Venus* and *early Mars* (Anglada-Escudé et al. 2013).
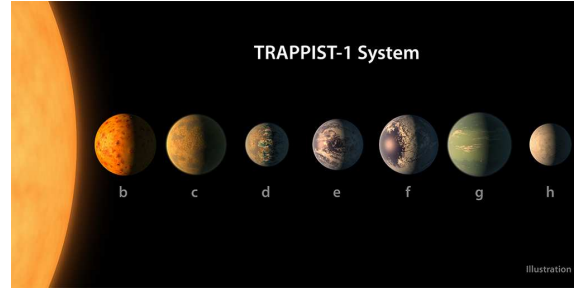

Fig. 18 Artistic picture of TRAPPIST-1 system (credit: Nasa/JPL-Caltech-R. Hurt and T. Pyle). Trappist-1d and Trappist-1e might potentially be within the HZ for this system.

habitability calculated by Lingam & Loeb (2017c) for planet e turns out to be at least one to two orders of magnitude lower than in the case of Earth.

8 General remarks

We wish to point out that the aim of previous sections was to consider the life as done, similar to what we know on Earth and of the kind considered in sect.2. Under this assumption, our goal was to explore some conditions for harboring and preserving it, and this determines the HZ limits, without any considerations about the origin of life. The introduction of climate model and its link with dynamics (sects. 5) is then consistent with our aim on this planetary scale, but some topics related to chapter on prebiotic chemistry and astronomy have been intentionally skipped. Nevertheless, let us mention something more of this very wide excluded perspective, at least for what is inherent to some aspects here considered. Ad example, in sect.2

one of the necessary request (δ)) for a site suitable for life was to allow formation of long molecular biological chains, with the implicit reference to polymer assembly. A very interesting mechanism has been applied by Lathe (2004, 2005) to biomolecules capable of association/polymerization at high salt concentration and of dissociation at low salinity. Nucleic acids like DNA meet these criteria. Lathe postulated that fast tidal cycling may be connected with the above request and also with the origin of life. At ocean shores tides may provide association/assembly on drying while charge repulsion on tidal dilution drive dissociation. If this mechanism really works that might suggest constraints on the evolution of extra-terrestrial life as Lingam & Loeb (2017a) claimed. They analyze the conditions under which tides may also exert a significant positive influence on abiogenesis and biological rhythms. Indeed most biological organisms on Earth have evolved internal timing mechanisms even though it is not clear if these kind of biological clocks are induced into life or they instead are key processes to obtain life.

8.1 Fast tidal cycling at the beginning of life

Whatever the answer may be it turns out interesting the comparison between what happens on Earth at origin of life and what is to be expected in some extra-Solar systems. It seems that the rotation period of the Earth was ~ 5 h at the time of Moon's formation (Brush, 1986). This rapid rotation might be due to the impact event that produced Moon (about 5 Gyrs ago). Moreover at the origin of life (about 3.9 Gyrs ago) the Moon was probably much closer to the Earth than present (perhaps only 200,000 km away) (Brush, 1986). As consequence, tidal forces were stronger than today and they also had a shorter period. According to Lathe (2004), large local fluctuations in salinity concentration could have provided effects on prebiotic precursor molecules and then also on the origin of life. Lingam & Loeb (2017a) argue about the possibility that something similar is also to be expected in planetary systems around low-mass stars (e.g., around the M star Gliese-667C, or TRAPPIST-1, an ultracool M dwarf (see sect. 7.2)).

9 Moving from CHZ toward GHZ and COSHZ

It is to noteworthy that the criteria adopted for establishing HZ run around only two necessary conditions (connected one to the other) in order to host life: to reach a reasonable surface temperature and to allow the presence of liquid water. These two conditions are met depending on the distance from Sun and on all the climatic factors which contribute to the greenhouse effect. However, we are dealing with necessary but not sufficient conditions. If we compare the requirements for the Earth to harbour life (sect.4), the conclusion is that some extra-Solar planets which lay within the habitable strip may not be really habitable (see also the remarks done in sect. 7.2, for the planets of TRAPPIST-1 system).

Moreover, in the next sections, we emphasize that to be sure a candidate lies within the HZ doesn't avoid the question: *in what part of the Galaxy is it located?*. Moving from the planetary scale (CHZ), the problem of the metal amount needed to form a planet like Earth, the threats of supernovae explosions and possible comet injections due to tidal Galactic effects, will force us to meet the wider chapter of Galaxy formation and evolution, introducing the Galactic Habitable Zone (GHZ). From that, in turn the horizon gets larger to the Cosmology because an interplay exists between some crucial factors constraining the main features of the Universe and its evolution with life. The set of these fine tuned links defines, in our view, the cosmological habitability (COSH) (sect.15).

10 Galactic Habitable Zone (GHZ)

In order to set some limits within the Galaxy for the birth and development of life, we first consider locations where it is possible to form Earth-like planets. The corresponding space-time location at Galaxy scale, suitable for life is constrained by the *metallicity amount* that the chemical-dynamical evolution of the Galaxy is able to yield.

Moreover to satisfy the requests γ) and δ) of sect.1, we have to protect life from supernovae explosions and injection of comets (sect.12 and 14.4).

In other words we at least have to take into account:

- the metal amount;
- the distance from Galactic center;
- the supernovae explosions;
- the Galactic tidal effects on an analog of our Oort's cloud, which might trigger a cometary bombardment towards the inner part of the planetary system.
- the time needed to develop a complex Life (already considered in sect.2).

A short historical synthesis about the limits of GHZ due to different authors, is given in Tab.1.

Introduced for the first time by Gonzalez et al. (2001)

the GHZ was essentially based on the metallicity gradient on the Galaxy disk. One of the more important factors is indeed the metallicity of the interstellar matter out of which a planetary system forms which determines the masses of terrestrial planets. The assumption was that lower metallicity led to smaller planets. So the upper limit for GHZ was estimated, very approximately, the Galactic location where the metallicity is, at least, half that of the Sun. The key issue was the production of terrestrial planets with a mass able to sustain plate tectonics (preliminary results about its dependence on the mass has been later on given by Noack & Breuer, 2011). The inner limit of this newly defined GHZ was set by high energy events. But the boundaries of GHZ remained not well defined.

Table 1 Limits of the Galactic Habitability Zone given by different authors. The time satisfies the request for complex life (see, next sections).

Time (Gyr)	Author	Limits
4-4,5	Gonzalez et al. (2001)	4.5-11.5 kpc
4,5	Lineweaver et al. (2004)	4-11 kpc
4,0	Lineweaver et al. (2004)	4-10 kpc
∼5,0	Prantzos (2006-2008)	5-16 kpc

10.1 Contribution of Lineweaver et al. (2004)

For defining better the GHZ they investigate the following items:

a)- the estimation of how many stars are available on the Galactic disk for hosting a planetary system. To this aim, the space-time trend for the *star formation rate* (SFR) has to be known.

b)- the lower and upper limits for the amount of the heavy elements which are necessary to build up a terrestrial planet. Too little metallicity means indeed a lack of necessary material to form a planet as Earth. Conversely too much of it would cause formation of a large number of massive planets, as we will see in sect. 11.2.1

To give the probability, P_{metals}, to host terrestrial planets, they need to know the space-time distribution of metals within the Galaxy. The answer is given in Fig.19, obtained by a chemical-dynamic model (Fenner and Gibson, 2003).

Moreover, they consider:

c)- the time needed for developing biological evolution. According to biological time clock of Fig.2 (item β)), a typical time of $4 \pm 1 Gyr$ is chosen. This constraint for complex life has been modeled as a probability, $P_{evol}(t)$, defined as cumulative integral of a gaussian distribution caracterized by a mean value of 4 Gyr with a dispersion of 1 Gyr.

As additional constraint, the necessity:

d)- to avoid the supernovae whose high energy radiations may be indeed very dangerous for life. The probability that complex life has to survive to this catastrophic event is defined as, $P_{SN} = 0.5 \, \xi(r,t)$, where $\xi(r,t)$ is a danger factor depending on Galactocentric distance r and on the time t of star formation.

At the end the relative number of potentially suitable planetary systems as a function of space and time, is given by:

$$P_{GHZ}(r,t) = SFR \cdot P_{metals} \cdot P_{evol} \cdot P_{SN} \qquad (10)$$

which means the composite probability of obtaining on Galaxy disk a site favourable for the development of complex life. The two factors P_{SN} and SFR are not independent (indeed as SFR decreases, P_{SN} increases). The GHZ is identified as the region in the disk bounded by the limit of 68% (until 95%) of $P_{GHZ}(r,t)$ (Fig.20). The above constraints define a zone centered around 8 kpc from the Galactic center growing with from 8 Gyr to 4 Gyr before present (*lookback time*) (Fig.20). By integrating $P_{GHZ}(r,t)$ over r we obtain the age probability distribution of complex life along the whole disk (on the right of Fig.20). This tells us that ∼ 75% of the stars that could harbor complex life in the Galaxy are older than the Sun of about 1 Gyr.

It is remarkable to note that (Fig.21):

- At the beginning of Galactic history the high star formation rate in the inner part of the disk (under 7 kpc and at about 8 Gyr, white arrow on the right) was able to produce heavy elements in order to form terrestrial planets but, at the same time, it caused, an unacceptable so high emissions from supernovae able to inhibit the rise of life during some Gyr (e.g. at 4 kpc, about 3 Gyr further must be spent, white arrow on the left).
- the Galactic bulge, which extends until about 3.5 kpc, turns out to be not an environment suitable for life because too crowded with stars and then potentially able to produce strong supernovae emissions and star encounters.
- As soon as the time constraint for reaching the evolution of complex life is relaxed, the Habitability Zone
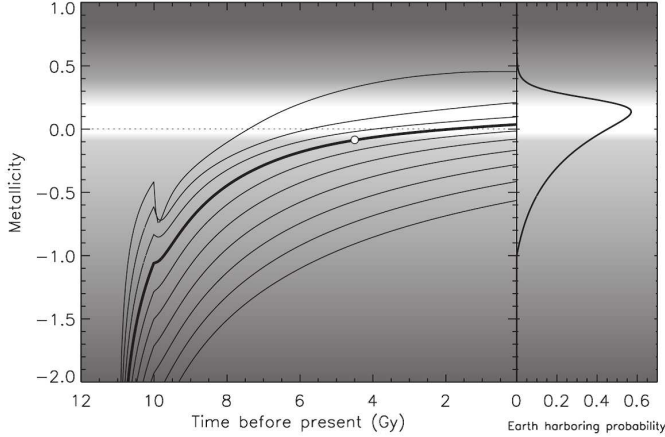
Fig. 19 Spatial distribution of metallicity at different Galactocentric distances from 2.5 kpc (upper curve) to 20.5 kpc (lower curve) with increments of 2 kpc, is shown as funtion of time. The white dot indicates the Sun's time of formation at Galactocentric distance of 8.5 kpc. On the right, the probability to harbour terrestrial planets as function of star host metallicity (based on chemical-dynamic model of Fenner and Gibson, (2003); see, Lineweaver et al., 2004).
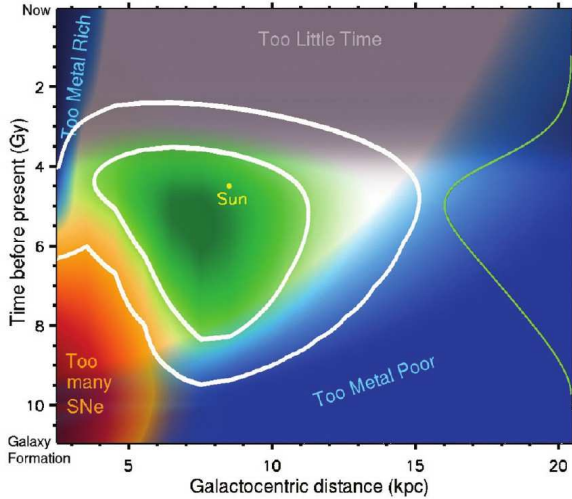
(68%) expands upwards, as shown in the lower picture of Fig.21).

In conclusion, from Lineweaver's et al. (2004) contribution two slightly different upper limits for the GHZ are obtained which depend on the different time needed to produce complex life (Tab.1): 11 kpc, in the case of 4.5 Gyr or 10 kpc, in the case of 4.0 Gyr. By relaxing the time constraint for developing complex life, the GHZ nowadays is in the range of about $4.5 \div 10\ kpc$ (Fig.21, lower panel).

Fig. 20 GHZ (in green) on Galaxy disk in the plot Galactocentric distance vs. *lookback* time, obtained by the requests based on the probability to harbour stars with suitable metallicity (blue region), with enough time for complex life evolution (gray region), and with freedom from life-extinguishing supernovae explosions (red region). The white contours encompass 68% (inner) and 95% (outer) of P_{GHZ}, including then the stars having the highest potential to be harboring complex life. The green line (on the right) shows the age distribution of the probability needed by complex life (see, text) (Lineweaver et al., 2004).
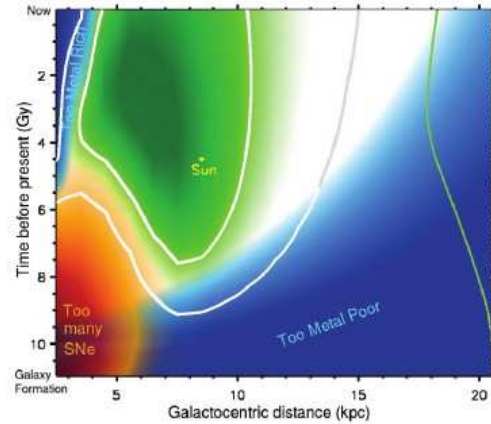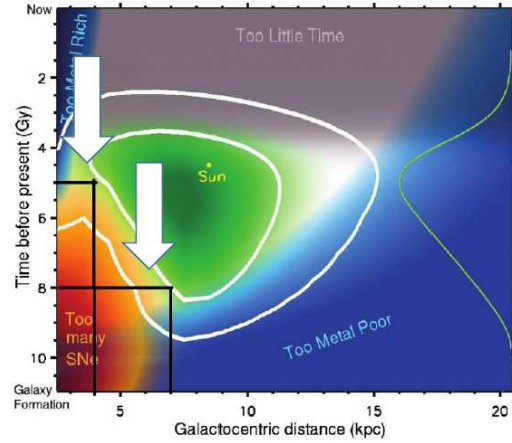

Fig. 21 GHZ as in Fig.20; see text for the meaning of the white arrows in the upper panel (Lineweaver et al., 2004, adapted by Fecchio, 2016). Variation of GHZ when the upper limit for the time to develop complex life is relaxed. Again, the green line on the right is the resulting age probability distribution of life along the whole disk (lower panel, Lineweaver et al., 2004).

10.2 Contribution of Prantzos (2006, 2008)

Prantzos is strongly critical about the limits given for GHZ by Lineweaver et al. (2004) being also very doubtful on the possibility to define them. In his opinion some assumptions which appear in Eq.10 are far from being unequivocally defined. He critically reviewed them.

10.2.1 Metal amount

To determine the metal amount two opposite requests have to be taken into account: the first is to have enough metals to form planets similar to the Earth, the other one is to avoid that the increasing metallicity produces also too many giant planets (so called "Hot Jupiters") whose masses are comparable (or superior) to that of Jupiter. In Fig. 22, the distribution function of planet vs mass (in Earth mass) is illustrated for three metallicity abundances of the central star and then of the proto-planetary disc. In principle, the gaseous giants form at a distance of several AU from their stars where the gas is available for accretion onto a rapidly growing rocky/icy core. By tidal interaction with the proto-planetary disk, they then lose angular momentum causing their inwards migration. During migration they may dynamically destabilize and eject from the system smaller planets which might host life.
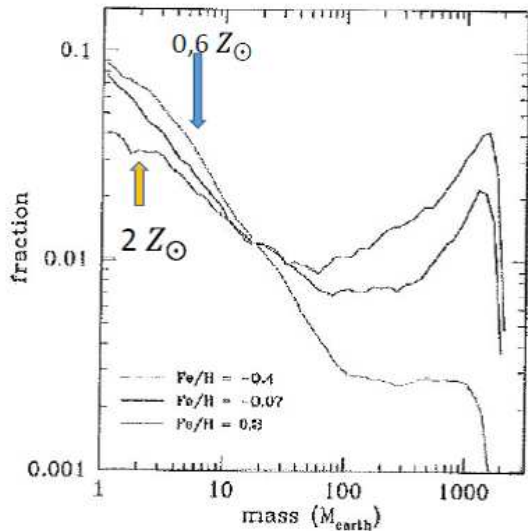

Fig. 22 Fraction of planets with different masses (in $M_\oplus$) which may form around a star of 1 $M_\odot$ as function of three different metallicity values for star (and corresponding proto-planetary disk) in the range ($0.6\ Z_\odot \div\ 2\ Z_\odot$). Increasing metallicity favours also the formation of giant planets (simulations of Mordasini et al., 2006).

In this scenario, we have to take into account not only the probability to form Earth-like planets but also to estimate the probability that they have to survive in presence of migrating giant planets (Fig.23). The resulting probability of having Earths surviving Hot Jupiters (HJ) is given as a function of Galactocentric distance at five different epochs of the Milky Way evolution: 1,2,4,8 and 13 Gyr, time-frames are shown on the last panel on the left of (Fig.23).

In addition, also the probability of surviving supernovae explosions has to be re-considered. Prantzos' opinion is that: if on the base of destructive effect of one SN explosion lies its capability to produce energetic particle/flux irradiation in order to induce a significant number of *gene mutations*, then one may calculate a lower limit for the distance (D) of the SN able to produce such fluxes/irradiations and an estimate of the Galactic SN frequency occurring at this distance. According to Gehrels et al. (2003), significant biological effects due to ozone depletion, i.e. doubling of the UV flux on Earth's surface, may arise for SN explosions closer than $D \sim 8pc$ with a frequency $f \sim 1Gyr^{-1}$ (evaluated by Prantzos). However Prantzos' opinion is that it appears hard to draw any quantitative con-
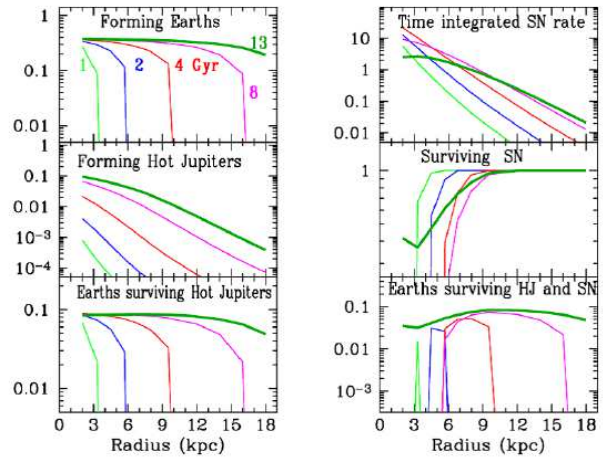

Fig. 23 Probabilities of various events as a function of Galactocenric distance at five different epochs of the Milky Way evolution: 1, 2, 4, 8 and 13 Gyr, respectively (the latter is displayed with a thick curve (green) in all figures). The probabilities of forming Earths is given in the upper left panel and of forming Hot Jupiters in the middle left one. To form Earths but also to survive the "Hot Jupiters" in the lower left panel , while the probability of life bearing planets surviving SN explosions is giving in the right middle panel. Finally, the overall probability for Earth-like planets surviving HJ and SN is shown on bottom right. Initially the GHZ defines a ring in the MW disk, progressively migrating outwards; that "probability ring" is quite narrow at early times, but fairly extended today and peaking at about 10 kpc (Prantzos, (2006-2008)).

clusions about the probability of *definitive sterilisation of a habitable planet* because, e.g. the considerations done are relative to all land animals whereas marine life could probably survive to a large extent (since UV is absorbed from a couple of meters of water). The overall probability to have Earths surviving HJ and SN at different Galactocentric distance and at different epochs is drawn in the last panel on the right of (Fig.23).

10.2.2 Prantzos vs. Lineweaver et al. 2004

Despite his perplexities, Prantzos gives the evolution of GHZ during the cosmological (universal) time, from 1 to 13 Gyr which is shown in final panel on the right of Fig. 23 . At 2 Gyr it appears as a very narrow ring of about $(4 \div 6)$ *kpc* (in blu) progressively growing at 4 Gyr to the extension of about $(5 \div 10)$ *kpc* (in red), reaching the dimension of about $(5 \div 16)$ *kpc* at 8 Gyr (magenta), including, practically now (13 Gyr), about the whole extension of the Galactic disk (thick curve in green). By comparing the results of Prantzos and Lineweaver's et al. (2004) and considering that they take into account the *lookback time* whereas Prantzos does not include the time needed for complex life, we can conclude that their strip at 4 Gyr may be assimilated with that of Prantzos at 8 Gyr (because it means allowing about 5 Gyr for complex life also in his approach), the Prantzos' GHZ turns out to be only slightly larger than that of Lineweaver et al. (2004), both having an increasing trend towards present. As soon as the term related to the time for developing complex life is relaxed (it means to consider for both the GHZ at the present) the difference between the two approaches are more relevant: for Prantzos the GHZ extension covers the whole disk with a maximum around 10 *kpc*, for Lineweaver's et al. (2004) the extension is only of $(4.5 \div 10)$ *kpc*.

We have also to point out that Prantzos (2006-2008) built up also probability isocontours of having an Earth-like planet surviving SN explosions in the time-distance plane. But because that refers to a planetary system around *one star* at a given time-space position, he multiplied this probability with the corresponding surface density of stars in order to obtain the probability of having life *per unit volume* in a given position. All that leads to the following paradoxial conclusion: despite the high risk from SN early on in the inner disk, this same place later becomes relatively "hospitable" because of large star density in it.

To similar conclusion arrive also Gowanlock et al. (2011). In such way the Solar neighborhood in the outer disk appears to be not privileged to host life whereas the more suitable environment for life appears to be in the inner disk with a probability peak at about 2.5 *kpc*.

10.3 A criticism

Against these two paradoxial conclusions which might leads to the drastic Prantzos' thinking that: *the concept of a GHZ may have little or no significance at all*, our criticism is the following: in his reasonings Prantzos takes into account the SN frequency which already needs implicitly the inclusion of SFR (conversely included explicitly by Lineweaver et al. (2004) in their probability Eq.(10)). Then probably Prantzos and Gowanlock's et al. last conclusions at the end of previous sect., are affected by considering two times the weight of the SFR.

That is the reason why we will continue to refer as a relevant proposal to the GHZ given by Lineweaver et al. (2004) improving it by adding the tidal Galactic effects on comets of Oort's Cloud or analog in extrasolar systems.

11 Galactic planar tides on the comets of Oort Cloud and analogs

The Oort's Cloud (Oort, 1950) is the natural reservoir for long period comets of our Solar System: it is an outer shell structure roughly placed between 20000 *AU* (~ 0.3 *ly*) and 150000 *AU* (~ 2.2 *ly*) from Sun.

The comets represent the remnants of the formation of our planetary system: they have been driven in the Oort cloud through a scattering process induced by proto-planets combinated with a Galactic tidal torque effect at the beginning of the history of the Solar System (Tremaine, 1993). The existence of other comet clouds in different planetary systems spread out in the Galaxy is suggested by recent evidences of dusty excess on debris disks in exoplanetary systems observed by Spitzer at 70 μm (Greaves & Wyatt, 2010). The Galactic tide may re-inject the Oort Cloud's comets towards the inner part of the planetary system producing a comet flux with possible impacts on it and then with consequences on the development of life.

The effects of the Galactic tides on the Oort Cloud's comets were studied by several authors (e.g., Heisler & Tremaine, 1986; Matese & Whitman, 1992; Fouchard et al., 2006). Usually they are separated into radial, transverse and orthogonal (to the disk plane) components. At solar distance from the Galactic center the orthogonal tide has been estimated to be about ten times more effective than the radial one, in perturbing the Oort Cloud's comets into the Solar System (Heisler & Tremaine, 1986; Morbidelli, 2005). At this distance, it appears to be the dominant perturber today and also

over the future long term (Heisler, 1990). In spite of that, the contribution of planar tides (radial and transverse) becomes non negligible when the distance of the parent star, with respect to the galactic center, changes, as shown by Masi et al.(2009) for the Oort cloud comets and by Veras & Evans (2013) in their analysis on dynamics for extrasolar planets. In particular the planar component of the tide may cause a great change if the central star decreases its distance and/or its mass with respect to the present solar one. Moreover they will certainly be non negligible in presence of spiral arm perturbations, as also Kaib et al. (2011) have already pointed out and it has been confirmed in the preliminary results of De Biasi (2014).

An interesting contribution to this problem comes out by the work of De Biasi et al. (2015). They consider only the effects of Galactic planar tides but at two different distances from the Galactic center: 4 kpc and 8 kpc, assuming the last one as the current solar position. That is performed in the perspective that the Sun may have migrated through the Galactic disk from an inner zone to the current one (Kaib et al., 2011) (sect.14). This means that the solar system could have been subjected to tidal perturbations stronger than those which characterize the present environment. The plastic impression has already been given in the paper of Masi et al. (2009). Indeed in their Fig.25, the effect of increasing total Galactic tidal perturbation moving toward the center of the Galaxy, clearly appears. In an inertial system of reference they studied the behavior of 48 test particles (simulating comets) with a common perihelion $q = 2000 \ AU$ and an increasing aphelion $a = (40, 60, 80, 100, 120, 140) \cdot 10^3 \ AU$, repeating each group at the following Galactic longitudes: $(0^o, 45^o, 90^o, 135^o, 180^o, 225^o, 270^o, 315^o)$ (Fig.24).

11.1 The contribution of dynamical Galaxy components to the tidal effects on comets

The main contributions to Galactic tide have their origin from the gravitational potential of the bulge $\Phi_{BG}(r)$, of the disk $\Phi_D(R, z)$ and of the dark matter halo $\Phi_{DH}(r)$ respectively given by (De Biasi et al., 2015):

$$\Phi_{BG}(r) = -\frac{GM_{BG}}{\sqrt{r^2 + r_c^2}} \qquad (11)$$

where M_{BG} is the bulge total mass, r_c is the *core radius* (Flynn et al., 1996) and G the gravitational constant, assuming as a good approximation the spherical model of the *Plummer sphere* (Binney & Tremaine, 2008).
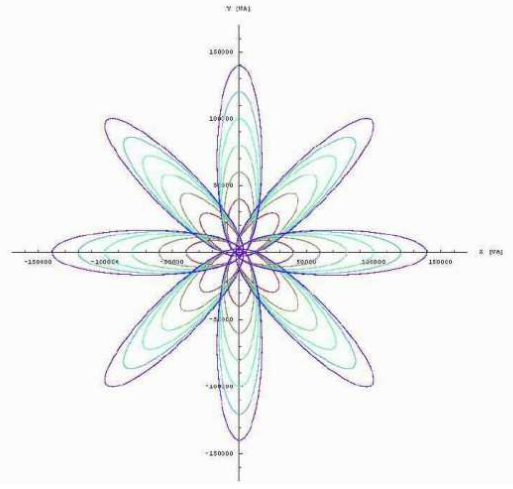

Fig. 24 Distribution of comet orbits in an inertial frame on the Galactic plane with the same perihelion and increasing aphelions at different Galactic longitudes (see text) before switching on the Galactic tides (Masi et al., 2003; Masi et al., 2009). The initial not perturbed orbits here considered are similar to those taken into account by De Biasi et al. (2015).
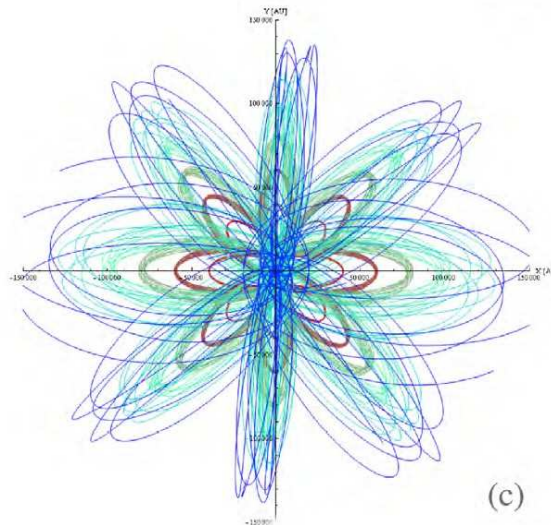

Fig. 25 As soon as Galactic tides are on, they affect the comet's orbits of Fig.24, as stronger as the Solar system is placed closer to the Galactic center (c), at 4 kpc (Masi et al., 2003; Masi et al., 2009).

For the *thin* axisymmetric disk the infinitely thin Freeman's model (Freeman, 1970) appears as main reference. But, in this context it is affected by some difficulties which may be overcame combining instead three Miyamoto-Nagai disks (Miyamoto & Nagai, 1975) of differing scale lengths and masses:

$$\Phi_{MN}(R,z) = -\sum_{n=1}^{3} \frac{GM_n}{\sqrt{R^2 + \left[a_n + \sqrt{b^2 + z^2}\right]^2}}. \quad (12)$$

The parameter b is related to the disk scale height, a_n to the disk scale lengths and M_n are the masses of the three disk combined components. It needs to stress that the potential trend given by Freeman's model results in fair agreement with that of (12) at the mid-plane ($z = 0$).

The Galactic mass distribution of the DM halo is still uncertain and there are several models in the literature. Instead of classical Navarro-Frenk-White (NFW; Navarro et al., 1997) density profile, the modified pseudo-isothermal (MPI) profile (Spano et al., 2008) is considered. That has been introduced to obtain the best fits of rotation curves in spirals and for LSB (low surface brightness galaxies), probably DM dominated. The corresponding gravitational potential is given by:

$$\Phi_{DH}^{MPI}(r) = -4\pi G \rho_0 r_H^2 \times$$

$$\left(\frac{\ln\left(r/r_H + \sqrt{1 + \left(\frac{r}{r_H}\right)^2}\right)}{r/r_H} - \frac{1}{\sqrt{1 + \left(\frac{R_{vir}}{r_H}\right)^2}} \right), \quad (13)$$

with ρ_0 the central dark halo density. The values of the constants a_n, b, M_n, according with Flynn et al.(1996), and the parameter values for each Galactic components are listed in Tab.1 of De Biasi et al. (2015).

11.1.1 Circular velocity and tide contributions from Galaxy components

The contributions to the total circular velocity trend vs. r from different Galaxy components are plotted in Fig. 26. The values for solar environment are inside the measured error bar for these distances (Klypin et al., 2002)

As we will see in the next sect., one relevant not expected result is the following: the contribution to the circular velocity coming from a dynamical Galactic component, enters in determinant way also the description of tide coming from the same component as soon as it is done in Hill's approximation (Eq.16). Because these contributions vary with the location of the Sun
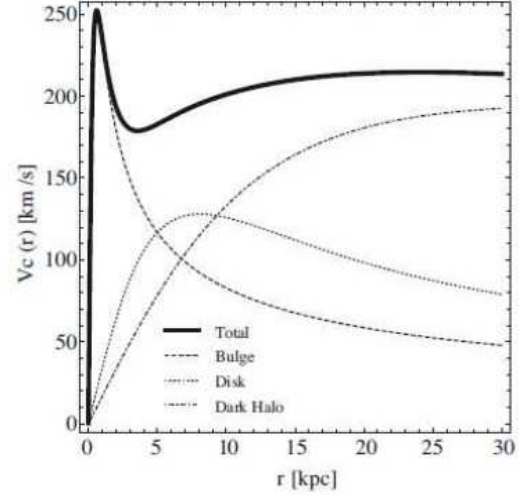

Fig. 26 The different contributions to the circular velocity vs the distance from the center are here plotted for Galaxy assuming a MPI density profile for DM halo (Spano et al., 2008) (De Biasi et al., 2015).

on the Galactic plane it turns out remarkable that one may predict what will be the Galactic component producing the most tidal effect on the Oort Cloud analogs around new extra solar planetary systems, simply looking at the position of its central star on the plot of Fig. 26.

11.2 On planar tide contributions in Hill's approximation

The Hill's approximation (Binney & Tremaine, 2008) adapts the formalism of the restricted three-body problem (i.e., Solar system, Galaxy, cometary body with mass very small in respect to the previous ones) for the case in which the dimension of satellite system (Solar system) is much smaller than its distance to the center of the host system (Galaxy). In our case the system Sun-comet indeed achieves the maximum size of 1 pc, while the distances from the Galactic center are about three orders of magnitude larger. In this situation the variation of the gravitational potential along the cometary orbits is very smooth, making possible the application of the *distant-tide approximation* (Binney & Tremaine, 2008, Chapt.8) . A solar co-rotating system which has the Sun as origin has been considered in this approximation developed for an axisymmetric potential also in 3D-dimensions by De Biasi et al., (2015). The analysis of the comet motion in this *synodic* system is taken into account. The x-y plane coincides to the stellar orbital plane, $\hat{\mathbf{e}}_{\mathbf{x}}$ points directly away from the center of the host system and $\hat{\mathbf{e}}_{\mathbf{y}}$ points in direction of the orbital motion of the satellite (Fig.27). The reference system rotates with the frequency $\mathbf{\Omega_o} \equiv \Omega_o \hat{\mathbf{e}}_{\mathbf{z}}$.

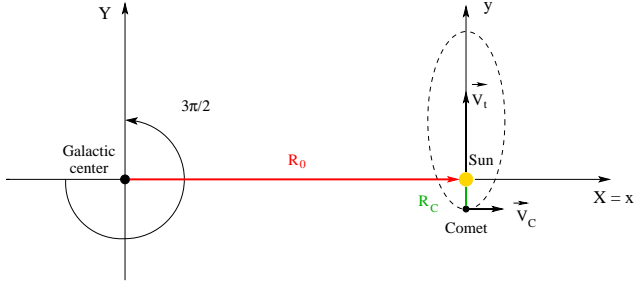The most relevant equation in it is the following one:

Fig. 27 Picture of the initial location for a comet orbit with galactic longitude $\frac{3\pi}{2}$ in the reference system with the origin on the galactic center (X,Y). The heliocentric system (x,y) (used in Hill's approximation) is also shown (De Biasi's et al.,2015).

$$\ddot{x}(t) = 2\Omega_0 \dot{y}(t) + [\Omega_0^2 - \Phi''(R_0)]x(t) - \frac{\partial \Phi_s}{\partial x}; \qquad (14)$$

giving the acceleration per unit mass of test particle at the point $x(t), y(t)$, along the x-axis. The first term on the right comes from the Coriolis' force, the last one is the contribution of Solar force, the middle one describes the variation of centrifugal force (term Ω_o^2 in square brackets) not completely in balance with the variation of gravitational force due to the host system (Galaxy, term $\Phi''(R_o)$) on the test particle position considered. Assuming a circular motion of the Sun around the Galactic center at the distance R_o and introducing the Oort's constants $A(R), B(R)$, the angular speed of Galactic rotation, measured at R_o is given by:

$$\Omega_o = A(R_o) - B(R_o) \qquad (15)$$

Then the x-component of tide from each Galactic i-component ($i = BG, D, DM$, bulge, disk, DM halo) is respectively given by:

$$\Omega_{oi}^2 - \Phi_i'' = (-2\Omega_i \Omega_i' R)_{R_o} = 2\frac{v_{ci}^2}{R_o^2}\left(1 - \frac{dln\ v_{ci}}{dln\ R}\right)_{R_o} \qquad (16)$$

The main result is that the x-component of Galaxy tide turns to be depending on the circular velocity contribution of each Galactic component and on its logarithmic gradient. Conversely the y-component turns to be zero due to the balance at Sun position: $\Phi'(R_o) = R_o\Omega_o^2$. That is one of the best results in De Biasi's et al. (2015) work: we know the tidal acceleration per unit length for each unit cometary mass coming from every dynamical component of Galaxy (Eq.16) before performing integration.

11.3 Effects of Galactic planar tide

One of the major effects of the Galactic planar tide on comet's orbit is the perihelion variation which may consist either in the precession of the major axis or in the variation of perihelion distance. The conditions that could amplify or reduce the effects of tidal perturbations turn out to be depending on the three main parameters: the star distance from the Galactic center, the Galactic longitude and the direction of motion of the comet's orbit.

11.3.1 Testing on comet's orbits

As exemplification, a test particle has been considered chosing a comet belonging to the outer shell of the Oort Cloud, where the solar gravitational force is lower and the galactic perturbations are then more evident. According to the differential distribution of the inverse semimajor axis for Long Period Comets of Oort's Cloud (Oort, 1950), with a spike at $3.7 \cdot 10^{-5} AU^{-1}$ corresponding to an aphelion of 54000 AU , the comet considered has initial aphelion of 140000 AU, initial perihelion of 2000 AU, inclination on the Galactic plane equal to zero, Galactic longitude equal to $\frac{3\pi}{2}$ and direct motion direction (Fig.27). Two distances are taken into account: 8 kpc and 4 kpc from the Galactic center.
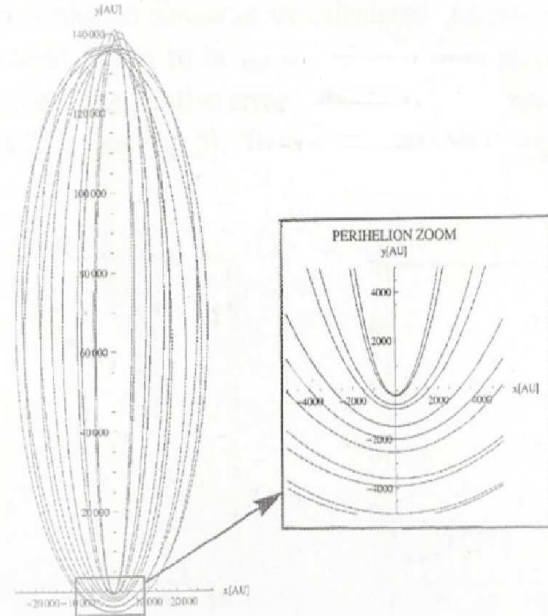

Fig. 28 Description of cometary orbits affected by Galactic tides in Hill's approximation when the central star is at 8 kpc from the center. Perihelion's zooms are also shown in the box (De Biasi, 2010).

As soon as the Galactic tidal effect is switched on zooms in perihelion zone (Fig.28) are performed distinguishing the contributions from the different dynamical Galactic components. A result in which the effect of bulge is dominant, appears in Fig. (29).
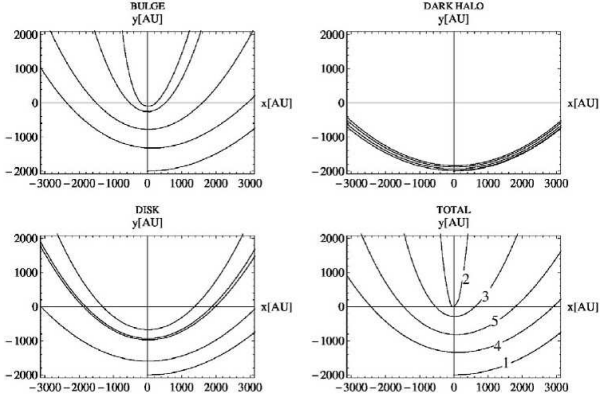

Fig. 29 Zoom of the perihelion zone for the comet's orbit considered at 4 kpc from the Galactic center (Hill's approximation). The most important perihelion's reduction is due here to the bulge. In an integration time of 1 Gyr, the global effect is to reduce perihelion's distance of 65%. The order of time-sequence is marked by numbers in the "Total" case (De Biasi's et al., 2015).

12 A new constraint on the GHZ

According to the previous result of sect.12.2, we are able to know the contribution to tidal acceleration per unit length and unit mass coming from each Galaxy's component only knowing the contribution of the component considered to the circular velocity (Fig.26), independently of the central star mass, longitude and direction of motion on comet's orbit. We only need the position of central star on the Galactic plane (Fig.30). Then it becomes very interesting to overlap this plot on that of Lineweaver et al., 2004 (Fig.20) in order to include a new relevant factor on the GHZ discussion (Fig.31). Using Fig.30 a quantification may be derived for Fig.31. We immediately may do, e.g. an estimation of the ratio, X, of the dominant tide coming from bulge, e.g., if Sun moves at 3 kpc, in comparison with that due to the dominant disk when Sun is, as now, at 8 kpc. X turns to be equal to 13.5. The same ratio becomes $X = 1.8$ as soon as the Sun was placed at 6 kpc, again under the dominant tidal effect from the bulge. Moreover, the relative amount of one Galaxy component over the other, may be given, e.g., at 4 kpc the tidal bulge effect surpass that of the disk at the same position of a factor of about 50.

In conclusion, if Sun during its probable past migration reached a location on Galactic plane under 7 kpc, the strong dominating tide from the bulge was probably able to induce cometary injection toward the inner part of the planetary system, producing a cometary flux with possible impacts on it. If Sun conversely remained in the range $7-15$ kpc it would have felt a lower tidal effect from the disk and over 15 kpc an even weaker effect from DM halo. The considerations are worth also for analog extra solar planetary systems.
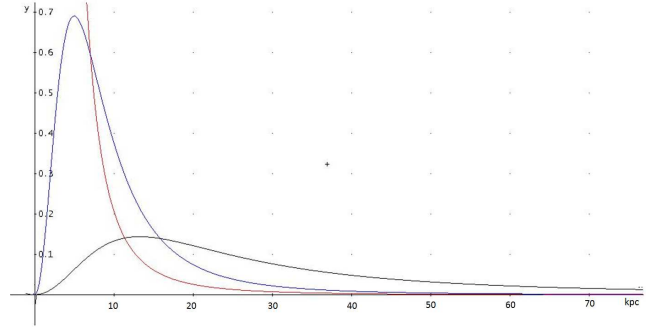

Fig. 30 Tidal acceleration from Galaxy components for unit length and unit mass (x-component, Eqs.14,16): from bulge (red), disk (blue), DM halo (dark), vs distance from the Galactic center (in kpc), using the contributions of Fig. 26. Bulge dominates until about 7 kpc, disk in about the range: $7-15$, DM halo over 15 kpc. An amplification factor of 10^3 has been used along ordinate axis (De Biasi et al., 2015).
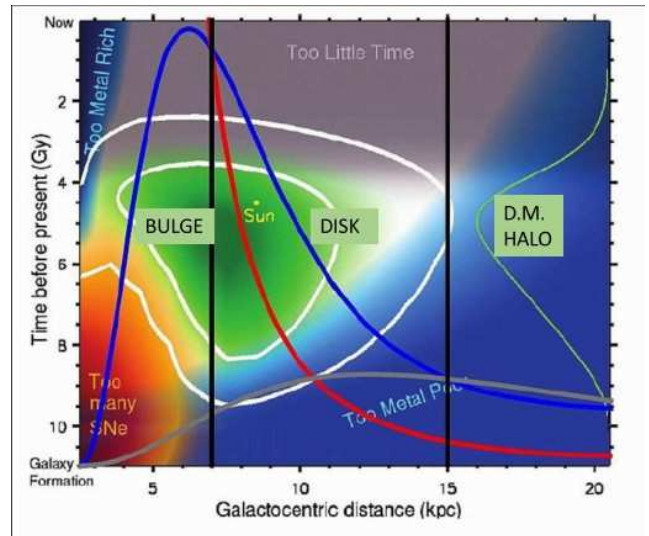

Fig. 31 Overlapping of the plot (Fig.30) on the Fig.20 given by Lineweaver et al. (2004). A new relevant factor is added in order to define the GHZ. The domains of different Galaxy components on tide are marked by vertical lines (Fecchio, 2016).

13 On probable solar path through the Galaxy

An important question is: in which location within the Galaxy the Sun formed? The Sun's metallicity actually seems to be over the mean value (of about 20% in Z) at the current Sun's position as derived from the mean metallicity gradient in the Galactic thin disk (Fig.32). This suggests that the Sun could actually be born at a shorter distance from Galactic center and that it may have undergone migration toward its present location. But how is it possible to reconstruct its path only on the basis of metallicity distribution on the disk?

13.1 On the metallicity gradient of Galactic thin disk

Theoretically speaking, to get the metallicity gradient of Galaxy disk is not an easy task. The simplest model has to deal with : i) the history of formation of a disk Galaxy inside the cosmological environment, ii) its dynamical evolution, iii) the local star formation prescription, iv) the standard chemical evolution once assumed a given initial mass function, and a model for spectral evolution of stellar populations.

If on one side the description of so many physical processes composing the whole picture requires the introduction of many parameters, from the observational point of view there is a very large spread in the data which is perfectly consistent if stellar migration occurred across significant galactocentric distances. Scattering with transient spiral arms (Roškar et al., 2008 a) and b)) might have caused it. Paradoxically, the description of Sun's migration meets an intrinsic barrier from observations.

There are indeed many good models considering the cosmological, dynamical and chemical evolution (Pagel, 1997; Prantzos and Silk, 1998; Portinari and Chiosi, 1999; Chiappini et al., 2001; Fenner and Gibson, 2003; Naab and Ostriker, 2006; Piovan et al. 2011) which are able to reproduce in a self-consistent way the mean metallicity distribution function (MDF) and the age-metallicity relationship (AMR). However, there is evidence that a large amount of scatter is present in the observed AMR of field stars and open clusters probably due to the superposition of stellar migration.

The overall observational uncertainties, which enormously increase considering the different chemical species (see, e.g., Table 1 in Portinari & Chiosi, 1999), give the impression that to refer to one experimental mean metallicity gradient could be meaningless.

In spite of that the different models considered lead to an intrinsic self-consistency, i.e., they are able to point out a mean value for the metallicity gradient on the
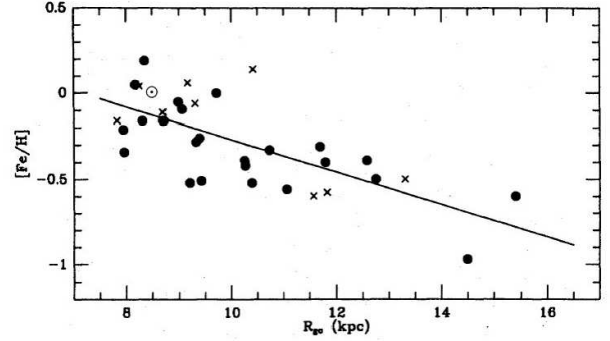

Fig. 32 Metal abundance gradient in the Galactic disk for open clusters older than 1 Gyr, filled circles are from Friel & Janes (1993), crosses from Lynga (1987). The line corresponds to the linear least squares fit equal to -0.095 ± 0.017 dex/kpc (Pagel, 1997, pg.93). Sun's position is also given.

disk without a so large spread among the models. In order to make a reasonable exercise on Sun's migration we assume that this consistency is really founded representing something intrinsic of disk as soon as we subtract the next occurrence of migration.

As reference we adopt the paper of Naab and Ostriker (2006) (NaO, hereafter) and compare their results with other relevant contributions to the topic, in particular that of Lineweaver et al. (2004) (LiN, hereafter) referring to the Galaxy evolution model of Fenner & Gibson (2003).

NaO obtain, at the present time, a mean metallicity gradient nearby the Sun, for gas (not too much different from that of stars) equal to:

$$\frac{dlogZ}{dR} = -0.046 \ dex \cdot kpc^{-1}$$

The result is about the same given by LiN (interpolation of their Fig.1), leading to a mean value:

$$\overline{\frac{dlogZ}{dR}} = (-0.05 \pm 0.01) \ dex \cdot kpc^{-1},$$

They both predict that the gradient was significantly steeper in the past at epoch of solar system formation, with a fairly good agreement. The mean value[3] between them turns out to be:

---

[3]It should be noted that also the observed mean logarithmic gradient of oxygen over H for Galactic HII regions, is believed by Pagel (1997, pgs. 93, 227) to be: $-0.07/dex \cdot kpc^{-1}$. The same value is also given by Mo et al. (2010, pg.542) to characterize the trend of Milky Way metallicity. In the first determination of GHZ this value has also been used by Gonzalez et al., 2001.

$$\overline{\frac{dlogZ}{dR}} = (-0.07 \pm 0.01) \ dex \cdot kpc^{-1}$$

By considering the lower and upper limits of both mean gradients and their accuracy, an average over-metallicity of about 0.1 dex yields a possible range for the initial Sun's position given by:

$$R_{i\odot} = 5.5 \div 6.7 \text{ kpc}$$

By inspecting Fig.20 we notice that the lower value of the initial Sun's position does not represent a problem because it is within the GHZ given by Lineweaver et al. (2004). The only warning comes from tidal trends of Fig.30. It indeed appears in Fig.31 that under 7 kpc the tide due to the bulge increases dramatically, causing probably a strong comet bombardment at the beginning of this assumed Solar path.

13.2 To look for possible migration of Sun-like stars

Kaib et al. (2011) used Galaxy simulations to approximate the dynamics that Sun-like stars may have experienced during the past 4 Gyr in the Milky Way starting from the epoch at which the Sun was born. The key ingredient for the processes there described is the presence of transient spiral arms. Solar analog stars at the last timestep of simulations, which starts at $t = 10 \ Gyr$, are choosen on the basis of stellar age, position, and kinematics (see, Fig.34).
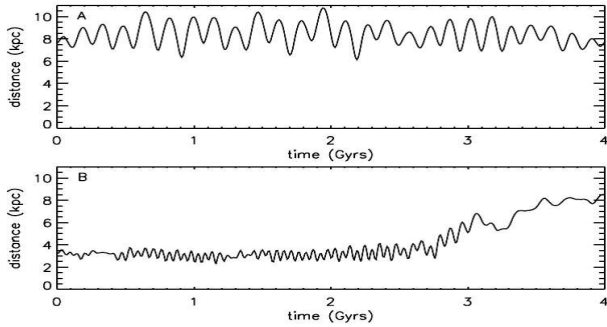

Fig. 33 Dynamical history for two solar analogs. One (case A) starts at 8 kpc at the beginning of simulation and comes back to the same orbital distance at the end of it, oscillating during the last 4 Gyr between 6 and 10 kpc. The other one (case B) spends most of its first 3 Gyr orbiting between $2.5 - 3.5$ kpc from the Galactic center and finally migrates outward to 8 kpc in the last Gyr of its history (see, text) (Kaib et al., 2011).

The set of solar analogs dispays a large variety of orbital histories.Two of them are shown in Fig.(33 A,B).

stars	age (Gyrs)	r (kpc)	z (pc)	u (km/s)	v (km/s)	w (km/s)
Sun	4.57	8.4 ± 0.6	25	10	18 ± 2	7.2
Sun Analogs	4.45 ± 0.15	8.05 ± 0.7	0 ± 100	0 ± 15	0 ± 15	0 ± 15

Fig. 34 Comparison between the kinematical properties of Sun and those of solar analogs in the Kaib et al. (2011) simulations. Solar distances to the Galactic center and above the midplane so as Solar velocity data are taken from references given in Kaib et al., 2011.

13.3 Overlapping possible migration paths on GHZ

In the Fig.35 the potential paths A and B obtained by simulations of Kaib et al. (2011) for two Sun's analog stars are superimposed to the GHZ of Lineweaver et al. (2011). The case A (shown on the left) which does not take into account the Sun's initial position due to its over-metallicity, turns out to be compatible with the requests of complex life (and, a fortiori, of not complex). Conversely, case B (on the right) which makes extreme the condition of over-metallicity, appears to be completely in disagreement with the conditions required for developing complex life. Only not complex life is compatible with this path in the last Gyr. However it holds again the warning related to shorter distance than 7 kpc, seen in sect.14.1, for possible comet's flux during more than the first 3 Gyr.
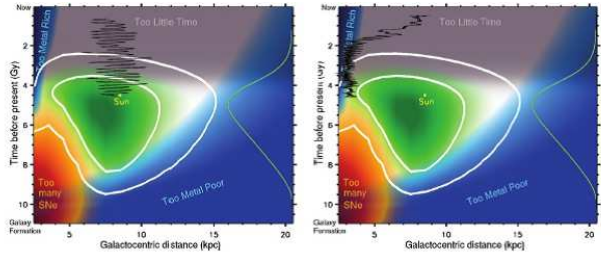

Fig. 35 Possible migration paths A and B of Kaib's et al. (2011) simulations are superimposed on the GHZ plot of Lineweaver et al. (2011). Path A, on the left, appears to be compatible also with complex life whereas path B, on the right, does not (see, text). The truncation at the end of both paths is due to the shorter age assumed for Sun (4 Gyr) in the simulations (see, De Biasi, 2014).

13.4 Comet's injection and the problem of water

A conclusion about the path B and, in general, about the exclusion of possible locations for planetary systems at distances shorter than 7 kpc, due to the stong tidal effect from bulge, cannot be definitively drawn at present time. If a comet's flux toward the inner planets

may indeed be produced at these distances, not necessarily it turns out to be dangerous for life but, conversely, it could be necessary for the developing of life. In fact it is still an open problem (Galletta & Sergi, 2005; Fecchio, 2016): which is the origin of the huge amount of water present on Earth?

The high temperature of the protoplanetary disk where the Earth formed (at about 4.5 Gyr from now) prevented the accretion of large amounts of water. It was probably accumulated later on due to impacts of minor bodies. Asteroids and Jupiter Family Comets appear the most promising candidates for delivering water to the Earth (Fig.36) even if the amount carried by asteroids might be much less in comparison with that from comets. The discriminating factor is the ratio D/H (deuterium over hydrogen)[4] which would rule out comets from Oort's Cloud but also some belonging to the Jupiter Family like the well studied comet 67P/Churyumov-Gerasimenko. The Orbiter Spectrometer for Ion and Neutral Analysis (ROSINA) on board of spacecraft Rosetta (ESA mission 2004-2016) measured for it a D/H ratio about three times greater than that on Earth. Also for the comet Hale-Bopp (1997; period of 2534 yrs) coming from Oort's Cloud and studied by Giotto spacecraft, its ratio turns out to be about two times that of Earth oceans. Conversely the spectral analysis performed by the spatial telescope Herschel (ESA) on comet Hartley 2 (103P/Hartley; period of about 6.5 yr) of Jupiter Family coming from the Kuiper's Belt, has given a ratio D/H more compatible with that on Earth (Fig.36).

In the context of bodies coming from Kuiper's Belt, the presence of a giant planet on an external orbit may be considered either positive or negative. It may act as a shield against an intense cometary flux due to the presence of an external perturber exciting cometary eccentricities. In this scenario, like in the solar system, an external planet (Neptune) may perturb an outer planetesimal belt (the Edgeworth-Kuiper belt) and inject icy bodies in the inner regions of the planetary system. These excited bodies might constantly impact a terrestrial planet orbiting close to the star possibly in the habitable zone. However, a giant planet like Jupiter can reduce the probability of impact of these planetesimals/comets on the inner body by increasing their inclination. The impact probability is diminished being inversely proportional to the $sin(I)$. On the other hand, if an external perturber(s) capable of stirring the bodies of an outer planetesimal belt is not present, a giant planet is not needed to protect the inner terrestrial

planets. However, in this case the delivery of water from the outer region of a protostellar disk becomes problematic and only the migration of the planet by tidal interaction with this disk, exchanging angular momentum, may drive a water rich terrestrial planet, formed in the outer parts of the disk, within the habitable zone. Planets formed in situ would be mostly rocky and possibly poor in water.
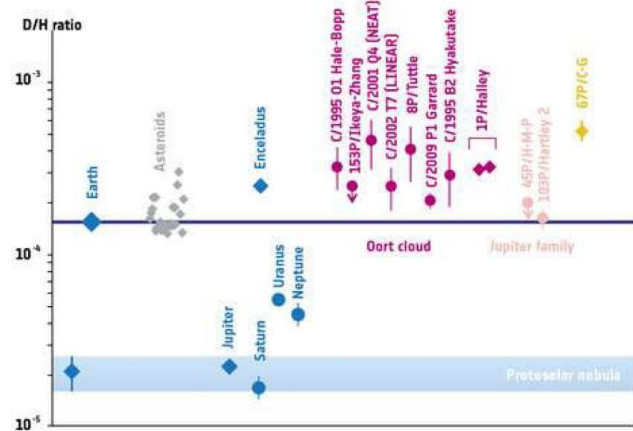

Fig. 36 Comparison of values of D/H ratios in different objects in the Solar System, grouped together by color: planets and satellites (blue), chondrites in the asteroid belt (grey), comets from the Oort Cloud (violet), and Jupiter family comets (pink). The comet 67P/Churyumov-Gerasimenko (yellow) has a different D/H ratio from the other comets in the same family. Horizontal line corresponds to the ratio for terrestrial oceans. (Credit: B. Marty/ESA/Altwegg et al., 2014; see, Fecchio, 2016).

14 Cosmological Habitability (COSH)

We don't refer, obviously, to a special, privileged location of the human being within the Universe, because the Copernican Principle holds[5]. We only suggest that it exists: *a collection of facts (sect.14.1) which connect the factors - constraining the main features of cosmos and its evolution- with life, by which it is possible to infer how strongly the life phenomenon is depending on these factors.* We refer to it as WRAP (Weak Reformulated Anthropic Principle; see, Secco, 2009).

---

[4] A still open problem is also if the ratio measured in the present ocean water was the same also in the past.

[5] As consequence of Cosmological Principle it follows indeed that from a physical point of view: *We are not priviliged observers of the Universe* (e.g., Peacock, 1999).

14.1 Interplay between the cosmological scenarios and the development of life

First of all we have to stress the principal factors which constrain the main features of the Universe. Briefly we can group them into the three following sectors (see, Dallaporta & Secco, 1993):

-A) the values of the main constants in Fundamental Physics.

-B) The global properties of the universe and its history (e.g., how it expands, how it builds up the chemical elements, etc).

-C) The space dimensionality.

They then need the link with the essential requests for life already considered in sect.2.

Generally speaking, a huge collection of relationships proposed by many authors (e.g.,Barrow & Tipler, 1986; Dallaporta & Secco, 1993; Rees, 2002; Barrow, 2003; Gingerich, 2007; Secco, 2009) may prove the interplay between the present cosmological scenarios and the development of life. Here we will take into account only few exemplifications for the sectors A) and B) inviting the reader to refer at the references cited above. The same holds also for understanding how special is the spatial dimensionality (C)) equal 3 of our universe, we will not consider here.

14.1.1 A) The values of the main constants in Fundamental Physics

We will here refer only to the coupling constant[6] values of the four fundamental forces: α_G (gravitational); α (electromagnetic); α_W (weak); α_S (strong) (Lederman & Schramm, 1989). The advantage to introduce them lies in the fact that the intensities of corresponding forces are expressed in adimensional terms allowing immediately their comparison. At ordinary energies their values turn out to be: $\alpha_G \simeq 10^{-39}$, $\alpha \simeq 7.3 \cdot 10^{-3}$, $\alpha_W \simeq 10^{-5}$, $\alpha_S = 15$. In Fig.37 their trends are given for increasing energy going toward singularity. Even if the reliability of the physical phenomena is decreasing, going in this direction, the *electro-weak unification* proved at about 100 GeV at CERN (Ginevra), allows us to take seriously into account the other possible unification as depicted by the grand unified theory (GUT) at the time of about $\sim 10^{-35} sec$. At this time, when the energy density of the universe had to be about $10^{15} GeV$, according to GUT the three forces: the *strong* and the *electro-weak* could be unified. The

spontaneous breaking of the high level symmetry corresponding to this unified force, occurred owing Universe's expansion, allowed the strong force to separate from the *electro-weak* and to assume a coupling constant which now is equal to: $\alpha_S \simeq 15$. At about $\simeq 10^{-11} sec$ the *electro-weak* symmetry broke too and the corresponding unified force splits into the *electro-magnetic force* (with a typical coupling constant value of, $\alpha \simeq 1/137$) and into the *weak* one (with a typical coupling constant of, $\alpha_W \simeq 10^{-5}$).

These values with which the forces detached differing one from the other, are crucial in the primordial nucleosynthesis epoch ($\simeq 200 sec$). Indeed if α_S increases only by 0.3%, *dineutron* binds and with, $\Delta\alpha_S/\alpha_S$, increasing by 3.4% the *diproton* is bound too. But if, $\Delta\alpha_S/\alpha_S$, decreases less than 9%, the deuterium nucleus fails to be bound (Davies,1972 in Barrow & Tipler, Chapter 5, 1986, pg. 322). These little changes might have catastrophic consequences for life. For example, if the deuteron was unbound, the consequences for the nucleosynthesis of elements necessary for development of Biology, are strong because *a key link in the chain of nucleosynthesis would be removed* (Barrow & Tipler, Chapter 5, 1986). Conversely if the strong interaction was a little stronger, the *diproton* stable bound state would have the consequence that *all the hydrogen in the universe would have been burnt to ^2He (diproton) during the early stages of the Big Bang and no hydrogen compounds or long-lived stable stars would exist today* (Barrow & Tipler, Chapter 5, 1986, pg. 322). Indeed the reactions to form ^4He would find a channel about 10^{18} times faster in comparison with those without *diproton* formation. The hydrogen reserve would have been quickly consumed without allowing, e.g., the water formation.

Moreover the stability of a nucleus of a mass number A and atomic number Z hinges on a fine link between the strengths of electromagnetic and strong forces as follows:

$$\frac{Z^2}{A} \leq 49\Big(\frac{\alpha_S}{10^{-1}}\Big)^2\Big(\frac{1/137}{\alpha}\Big)$$

Thus, if the electromagnetic interaction were stronger (increased α) or a stronger interaction a little weaker (decreased α_S), or both, then biologically essential nuclei like carbon would not exist in Nature (Barrow & Tipler, Chapter 5, 1986, pg.326).

A long collection of other exemplifications of this kind are given in the cited book.

14.1.2 B) The global properties of universe and its history

We don't consider here the *fine tuned cosmological expansion* which constraints in a not trivial way the trend

---

[6]Actually they are not constant but function of energy to which they refer (see, Fig. 37).
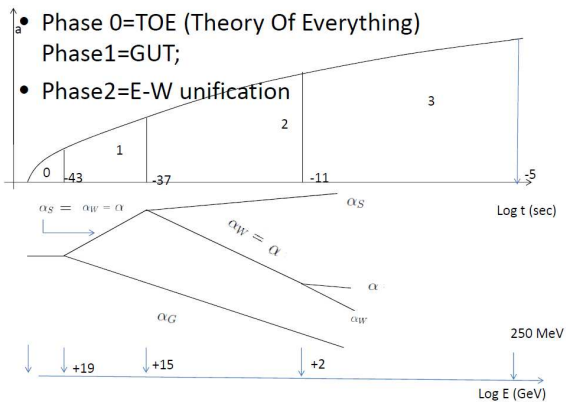
Fig. 37 Trends of coupling constants as function of time and energy during cosmological evolution (see, text). On the upper panel the development of expansion parameter is also shown, without inflationary epoch (elaboration from that given in Chapt.6 by Lederman & Schramm, 1989).

of density parameter Ω. That is strictly related to the age of Universe and to the possibility to form structures. Both are of course linked to the necessary conditions for life (e.g., Dallaporta & Secco, 1993). Neither we will refer about the mistery of the *fine tuning* related to the *cosmological constant* Λ. Nor we will take into account the interesting answer given by Rees (2002):*"its tuning....may be a fundamental request for our existence"*. Let us remember at least one of the many incredible bottle-necks through which the Universe's evolutive story passes. It refers to how the Universe build up the chemical elements, precisely how it occurs the production of the so large amount of carbon which life needs.

Carbon and Oxygen nucleosynthesis

After helium burning, inside stars of first generation, nucleosynthesis transforms three helium nuclei into one of carbon as follows: $3\,^4He \rightarrow\,^{12}C$. At first two helium nuclei collide producing the nucleus of ^8Be. But this nucleus is unstable and would decade in $\simeq 10^{-7}sec$ unless it captures a third helium nucleus in order to change itself into ^{12}C. But this chain at the reaction temperature of about 10^8K would not produce enough carbon for life unless the last reaction was resonant, that means there would exist a level of ^{12}C nucleus about equal to the intrinsic energy of the two nuclei $^8Be +^4 He$ plus the mean typical kinetic energy of collision at 10^8K, so that the reaction rate would increase strongly . The resonance level indeed exists and it corresponds to $7.6549\,MeV$, as Hoyle predicted since 1954. This resonance channel was soon verified by Fowler in the laboratory (e.g., Reeves, 1991, pg.61; Ortolan & Secco, 1996). He got the Nobel Prize (1983) also for

that. To be noted as Anthropic Principle (weak form, WAP) has again shown its prediction capability as a real physical principle must have.

It should be noted that the next reaction of carbon burning by which oxygen is produced has also to be tuned but in the opposite way. Indeed the following reaction: $^{12}C +^4 He \rightarrow^{16} O + \gamma$ must not to be resonant. If it does, all the carbon would be transformed into oxygen. Luckily it does not even if there is a resonant level for the oxygen nucleus but at slightly lower energy, $7.1187\,MeV$ (Dallaporta & Secco, 1993). So comparable quantities of carbon and oxygen are produced to make the CO molecule a common one. As consequence the formaldehyde H_2CO is simply the association of two of the most common molecules in the universe (H_2 and CO). Moreover molecules as:

$$(H_2CO)_n \rightarrow \; sugars \; and \; carbohydrates$$
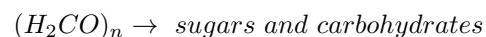
are easily built up (Hoyle, 1991).

To be noted that the carbon and oxygen energy nuclear levels are strictly depending on the values which α and α_S properly have. If α would vary more than 4% or α_S more than 0.4%, the carbon or oxygen production will change of a factor in the range $30-1000$ (Barrow, 2003).

15 Conclusions

Starting from the local scale, life leads to connect us with the largest scale, that of Universe. From this analysis a possible scenario arises in which links among the different scales are advanced. Even if possibly partial, a large set of minimum conditions has been identified which must be met for allowing life. The consequence of these conditions is that if we look at life from the probability point of view and then regard it as a complex phenomenon composed, by compatible and independent events, the probability to get it tends drastically to zero. But *we are*! With F. Hoyle we too may then do the following considerations: are we dealing with a *"monstrous sequence of accidents"*? Conversely *"...my apparently random quirks have become part of a deep-laid scheme.* [7]*"*

Moreover, regarding some complex phases of the cosmological evolution (e.g. the breakings of symmetries) it

---

[7] *"I do not believe that any scientist who examined the evidence would fail to draw the inference that the laws of nuclear physics have been deliberately designed with regard to the consequences they produce inside the stars. If this is so, then my apparently random quirks have become part of a deep-laid scheme. If not then we are back again at a monstrous sequence of accidents."* (Hoyle, 1959).

appear particularly surprising the direction they finally undertake (e.g. the corresponding values of coupling constants). Life will be connected to those values but life will be present only many Gyr later. Universe appears to have played a football game but without ball (=life). Whatever may be what one believes, there is some Beauty in all that, not too much different from what we experience in the current life, when we realize as the possibility to be live at any time is guaranteed by having our blood with many of its parameters together inside very strict ranges. Is really finely tuned the architecture within which life, as precious stone, is embedded.

Acknowledgements

16 Appendix

Nitrogen constitutes about 2.5% of the human body and about 78% of the Earth's atmosphere. It plays an essential role in the chemistry of life and it is one of the elemental building-blocks of amino acids. As a consequence, its compounds are fundamental for living organisms.

Where does this element come from? In stars of second generation during main sequence phase when the temperature inside is higher than about $15 \cdot 10^6 \ K$, by CN cycle. In it the mean reaction times differ from reaction to reaction enormously (e.g., ^{14}N has a reaction time twenty times longer than ^{12}C). Only when equilibrium is reached, each isotope is formed just as fast by one reaction as it is destroyed by another one. The equilibrium conditions, when the reaction rates per cubic centimeter must be equal for all six steps of the cycle, corresponds to this mass abundance ratios (Schwarschild, 1958):

$$\frac{X(^{14}N + ^{15}N)}{X(^{12}C + ^{13}C)} = 21 \pm 8$$

Then the carbon has to be decreased in favor of nitrogen (and oxygen) which becomes abundant within stars.

Another evolutionary phase in which carbon and oxygen too decrease in favor of nitrogen is during the AGB (asymptotic giant branch) for stars of $M \geq 4 - 5M_\odot$ by the CNO cycle. It involves two groups of reactions: the previous six of CN plus other nine when, $^{15}N + p$, opens the other low probability (1/2500) channel, going into $^{16}O + \gamma$, at an higher temperature of about $20 \cdot 10^6 K$ (Chiosi, 2012, pg.205; Galletta, 2012). During advanced evolutionary stages, it occurs indeed that H_e-burning in the core is exhausted and the energy star sources are located into two shells, the inner one by H_e-burning the outer one by H-burning. It follows some phases of three *dredge-up* phenomena, thermal pulses and mass-loss. Then the temperature on the basis of the convective envelope may become so high to start the H-burning by the CNO cycle via a process of HBB (*hot bottom burning*) which allows the star to become the most efficient source of nitrogen (Ferranti, 2015; Chiosi, 2012, pg. 379).

An other essential element for life is the phosphorous. In human body it represents about 1.1% of body weight. Most of it $(80 - 85\%)$ is in the skeleton while 1% in the brain. It is necessary for nucleic acids and it is involved (with also sulphur) in "high energy" bonds which can supply energy for biochemical reactions (Barrow & Tipler, 1986, pg.553). It enters indeed methabolic processes within the cells in particular in those transforming chemical into biological energy. Its percentage by weight in the lithosphere is

only of 0.12% (Barrow & Tippler, 1986, pg.542). That follows from the low abundance of P in the interstellar gas: about 2 atoms of P for each 100 millions of H atoms. The reason of this scarcity is connected with the nuclear synthesis mechanism of phosphorous which occurs by oxygen burning in the core of massive stars ($\geq 12\ M_\odot$) at temperature of about $1.5 \cdot 10^9\ K$ (Chiosi, 2012, pg.215; Galletta, 2012). Massive stars are indeed less numerous than the low mass ones.

Lingam & Loeb (2017b) have considered the perspective for life on planets with subsurface oceans (e.g., Europa and Encelado). The main idea they take into account is that planets lying ouside the HZ could not be precluded to life. One important aspect considered is that phosphorous must be available in the form of chemical compounds which have to be soluble and active in liquid water in order to supply the necessary energy for life. This would imply a geochemical phosphorous cycle which, e.g., on the Earth, has been done in the past by volcanic environments (Galletta & Sergi, 2005). Their conclusion is that this kind of crucial cycle faces challenges on these planets.

References

Altwegg, K., Balsiger, H., Bar-Nun, A., Berthelier, J. J., Bieler, A., Bochsler, P., Briois, C., Calmonte, U., Combi, M., De Keyser, J., Eberhardt, P., Fiethe, B., Fuselier, S., Gasc, S., Gombosi, T. I.,Hansen, K. C., Hassig, M., Jackel, A., Kopp, E., Korth, A., LeRoy, L., Mall, U., Marty, B., Mousis, O., Neefs, E., Owen, T., Reme, H., Rubin, M., Semon, T., Tzou, C.- Y., Waite, H., Wurz, P.. 67P/Churyumov-Gerasimenko, a Jupiter family comet with a high D/H ratio. Science, 2014.

Anglada-Escudé G., Tuomi. M, Gerlach E., Barnes R, Heller R., Jenkins J, Wende S, Vogt S., Butler P., Reiners A. & Jones R. H. A., A dynamically-packed planetary system around GJ 667C with three super-Earths in its habitable zone, A&A, N.556, A126, 2013.

Arney G., Domagal-Goldman S.D., Meadows V.S., Wolf E.T., Schwieterman E., Charnai B., Claire M., Hébrard E., and Trainer M.G., The Pale Orange Dot: The Spectrum and Habitability of Hazy Archean Earth, Astrobiology, 16, N.11, 2016.

Baltes H.P., On the validity of Kirchhoff's law for a body in nonequilibrium environment, Progress in Optics, 13, pp.1-25, 1976.

Barr A.C., Dobos V., and László L.K., Interior Structures and tidal heating in the TRAPPIST-1 planets, Astronomy & Astrophysics, 613, A37, 2018.

Barrow J. D. & Tipler F. J., The Anthropic Cosmological Principle, Oxford University Press, 1986.

Barrow J., I numeri dell'universo, Ed. Oscarmondadori, 2003.

Binney J. and Tremaine S., Galactic Dynamics, Second edition, Princeton Series in Astrophysics, 2008.

Breuer D. and Spohn T., Early plate tectonics versus single-plate tectonics on Mars: Evidence from magnetic field history and crust evolution, Journal of Geophysical Research: Planets, Volume 108, Issue E7, 2003.

Brush S.G., Early history of selenogony, in Origin of the Moon, Eds.: Hartmann W.K.,Philips R.J., Taylor G.J., Lunar and Planetary Institute, Houston,pp.3-15, 1986.

Chiappini C., Matteucci F.,Romano D., Abundance Gradients and the Formation of the Milky Way, ApJ, 554, 1044, 2001.

Chiosi C., Dispense di Astrofisica Teorica Mod. A, 2012.

Curtis H. & Barnes N. S., Invito alla biologia, Ed. Zanichelli, 1991.

Dallaporta N. & Secco L., Il Principio Antropico in fisica ed in cosmologia, Giornale di Fisica, Ed. Compositori Bologna, Vol. 34, N. 3, 163-192, 1993.

Davies P.C.W., J.Phys. A 5, 1296, 1972.

Davolio S., Dispense-radiazione, Institute of Atmospheric Sciences and Climate, Universitá Cattolica (Brescia), 2012.

De Biasi A., Tesi di Laurea Magistrale: Effetti Mareali della Galassia su orbite di proto comete della Nube di Oort, Relatore: Secco. L., Dipartimento di Astronomia di Padova, 2010.

De Biasi, A., PhD Thesis, University of Study of Padua, Supervisor Secco L., Advisors: Lunine J., Chernoff D., 2014.

De Biasi A., Secco L., Masi M. and Casotto S., Galactic planar tides on the comets of Oort Cloud and analogs in different reference systems, A&A, N. 574, A98, 2015.

De Pater I. & Lissauer J.J., Planetary Sciences, Cambridge University Press, 2001.

Fecchio M., Tesi Magistrale in Astronomia, Abitabilitá su scala locale, Galattica, cosmologica, Rel. Marzari F., Corr. Secco L., Universitá di Padova, AA. 2015-2016.

Fenner Y. and Gibson B.K., Deriving the Metallicity Distribution Function of Galactic Systems, Publ.Astron.Soc.Aust., 20, 189, 2003.

Ferranti F., Tesi in Astronomia, Il processo s in stelle AGB: Il problema del Rubidio, Rel. Marigo P., Universitá di Padova, AA. 2014-2015.

Flynn C., Sommer J. L. & Christensen P., Kinematics of the outer stellar halo, MNRAS, N. 281, 1027-1032, 1996.

Fouchard, M., Froeschlé, C., Valsecchi, G., & Rickman, H., Long-term effects of the Galactic tide on cometary dynamics Celestial Mechanics and Dynamical Astronomy, 95, 299, 2006.

Freeman, K. C., On the Disks of Spiral and S0 Galaxies, ApJ, 160, 811, 1970.

Friel E.D., Janes K.A., Metallicities and radial velocities of old open clusters, A&A, 267, 75, 1993.

Galletta G., Dispense di Astrobiologia, 2012.

Galletta G. & Sergi V., Astrobiologia, Le frontiere della vita, Ed. Hoelpi, 2005.

Gehrels N., Laird C. M., Jackman C. H., Cannizzo J. K., Mattson B. J., Chen W., Ozone Depletion from Nearby Supernovae, ApJ, 585, 1169, 2003.

Gillon M., Jehin E., Lederer S.M., Delrez L., de Wit J., Burdanov A., Van Grootel V., Burgasser A.J., Triaud A.H.M.J., Opitom C., Demory B.-O., Sahu D.K., Bardalez Gagliuffi D., Magain P., Queloz D., Temperate Earth-sized planets transiting a nearby ultracool dwarf star, Nature, 533, 221, 2016.

Gingerich O., Cercando Dio nell'universo, Lindau, 2007.

González, G.F., Forget F., Coll, M.A., López-Valverde, M.A., The Martian Upper Atmosphere, LNEA III, Eds: Ulla, U. & Manteiga, M., 2008.

Gonzalez G., Brownlee D. and Ward D., Una nicchia nella Galassie, Le Scienze, N. 398, 68-75, 2001.

Gonzalez G., Habitable Zone in the universe, Origins of Life and Evolution of Biospheres, N. 35, 555–606, 2005.

Gowanlock M., Patton D. & McConnella S., Model of Habitability Within the Milky Way Galaxy, Astrobiology, N. 11, 855-873, 2011.

Greaves, J. S., & Wyatt, M. C., Debris discs and comet populations around Sun-like stars: the Solar system in context, MNRAS,404, 1944, 2010.

Hauber E., Brož P., Jagert F., Jodlowski P., Platz T., Very recent and wide-spread basaltic volcanism on Mars, Geophysical Research Letters, Volume 38, Issue 10, 2011.

Hauck S.A., Phillips R.J., Thermal and crustal evolution of Mars,Journal of Geophysical Research: Planets, Volume 107, Issue E7, 2002.

Heisler, J., & Tremaine, S., The influence of the galactic tidal field on the Oort comet cloud, Icarus, 65, 13, 1986.

Heisler, J., Monte Carlo simulations of the Oort comet cloud, Icarus, 88, 104, 1990.

Hoyle F., Religions and the scientists, SCM, London, 1959.

Hoyle F., Il principio antropico e il pincipio cosmologico, a cura di Giacomini B., Ed. Spazio Libri Editori, 1991.

Kaltenegger L., Eiroa C. & Fridlund C. V. M., Target star catalogue for Darwin Nearby Stellar sample for a search for terrestrial planets, Astrophysics and Space Science, DOI 10.1007, 2010.

Kaib, N.A., Roškar, R., & Quinn, T., Sedna and the Oort Cloud around a migrating Sun, Icarus, 215, 491, 2011.

Kane S. R., Hill M. L., Kasting J. F., Kopparapu R. K., Quintana E. V., Barclay T., Batalha N.M., Borucki W. J., Ciardi D. R., Haghighipour N., Hinkel N. R., Kaltenegger L., Selsis F., Torres G., A Catalog of Kepler Habitable Zone Exoplanet Candidates, ApJ, 830, 1, 2016.

Kasting J.F., Toon B. & Pollack J., L'evoluzione del clima sui pianeti terrestri, Le Scienze, N. 236, 56-67, 1988.

Kasting J.F., Whitmire D. P. & Reynolds R. T., Habitable Zones, Icarus, N. 101, 108-128, 1993.

Kasting J.F., Kopparapu R., Ramirez R.M., & Harman C.E., Remote life-detection criteria, habitable zone boundaries, and the frequency of Earth-like planets around M and late K stars, PNAS, 111, 12641, 2014.

Klypin A., Zhao H. and Somerville R., CDM-based Models for the Milky Way and M31. I. Dynamical Models, ApJ, N. 573, 597-613, 2002.

Knoll A.H. & Nowak A., The timetable of evolution, Sci.Adv., Review, 3, 2017.

Kopparapu R., Kasting J., Ramirez R., Eymet V., Robinson T. D., Mahadevan S., Terrien R. C., Goldman S. D., Meadows V. & Deshpande R., Habitable Zones Around Main Sequence Stars: New Estimates, ApJ, N. 765, 131, 2013.

Kopparapu R. K., Ramirez R., Kasting J.F., Eymet V., Robinson T. D., Mahadevan S., Terrien R. C., Domagal-Goldman S., Meadows V., Deshpande R., Habitable Zones Around Main Sequence Stars: New Estimates, ApJ, N. 770, 82, 2013c, Erratum.

Kopparapu R., Ramirez R., SchottelKotte J., Kasting J., et al., Habitable Zones around Main-sequence Stars: Dependence on Planetary Mass 2014, ApJL, 787,L29.

Laskar J. and Robutel R., The chaotic obliquity of the planets, Nuture, 361, 608, 1993.

Lathe R., Fast tidal cycling and the origin of life, Icarus, N.168, 18-22, 2004.

Lathe R., Tidal chain reaction and the origin of replicating biopolymers, Int.J. Astrobiol., 4(1), 19-31, 2005.

Lederman L.M., Schramm D.N., From Quarks to the Cosmos, Tools of Discovery, Scientific American Library, 1989.

Lineweaver C. H., An Estimate of the Age Distribution of Terrestrial Planets in the Universe: Quantifying Metallicity as a Selection Effect, Icarus, N. 151, 307-313, 2001.

Lineweaver C. H., Fenner. Y. & Gibson B. K., The Galactic Habitable Zone and the Age, Le Scienze, N. 303, 59–62, 2004.

Lingam M. & Loeb A., Implications of tides for life on exoplanets, arXiv:1707.04594v2, 14 Nov 2017a.

Lingam M. & Loeb A., Subsurface Exolife, arXiv:1711.09908v1, 27 Nov 2017b.

Lingam M. & Loeb A., Physical constraints on the likelihood of life on exoplanets, arXiv:1707.02996, 07/2017c.

Lynga G., Distribution of OB associations and open star clusters, in: European Regional Astronomy Meeting of the IAU, 10th, Prague, Czechoslovakia, Aug. 24-29, 1987, Proceedings. Volume 4 (A89-32590 13-90). Ondrejov, Czechoslovakia, Czechoslovak Academy of Sciences, p. 121-127, 1987.

Marzari F. & Vanzani V., Dispense del corso di Fisica dei Pianeti, 2012-2013.

Masi M., Secco L. and Vanzani V., Dynamical effects of the Galaxy on the Oort's Cloud, Mem. S.A.It, N. 74, 494-495, 2003.

Masi M., Secco L. and Gonzalez G., Effects of the planer galactic tides and stellar mass on comet cloud dynamics, The Open Astronomy Journal, N. 2, 74-89, 2009.

Matese, J.J., & Whitman, P. G., A model of the galactic tidal interaction with the Oort comet cloud, Celestial Mechanics and Dynamical Astronomy, 54, 13, 1992.

Mischna M.M., Kasting J.F., Pavlov A.A., & Freedman R., Influence of Carbon Dioxide Clouds on Early Martian Climate,Icarus, 145, 546, 2000.

Miyamoto M. and Nagai R., Three-dimensional models for the distribution of mass in galaxies, Publications of the Astronomical Society of Japan, N. 27, 533-543, 1975.

Mo H., van den Bosch F., White S., Galaxy Formation and Evolution, Cambridge University Press, 2010.

Morbidelli A., Origin and Dynamical Evolution of Comets and their Reservoirs, arXiv:astro-ph/0512256, 2005.

Mordasini C., Alibert Y. and Benz W., Proc. Tenth Anniversary of 51 Peg-b: Status of and prospects for hot Jupiter studies, Paris: Frontier Group, N. 84, 2006.

Naab T. & Ostriker J.P., A simple model for evolution of disc galaxies: the Milky Way, MNRAS, 366, 899-917, 2006.

Navarro, J.F., Frenk, C. S., & White, S. D. M., A Universal Density Profile from Hierarchical Clustering, ApJ, 490, 493, 1997.

Neron de Surgy O., Laskar J., On the long term evolution of the spin of the Earth, A&A, 318, 975, 1997.

Noak L. & Breuer D., Plate tectonics on Earth-like planets, EPSC-DPS Joint Meeting, Vol.6, 890, 2011.

Oort J., The structure of the cloud of comets surrounding the Solar System and a hypothesis concerning its origin. Bull. Astronomical Institute of Netherlands, N. 11, 91-110, 1950.

Ortolan A. and Secco L., Il principio Antropico fra dominio della Scienza e quello della filosofia, Giornale di Fisica, 37-4, Ed. Compositori, Bologna, 1996.

Ortolani S., Dispense di Astrofisica Generale Mod. A, 2012.

Palen, S., Kay L., Smith, B., Blumenthal, G., 2011. Understanding Our Universe. New York: W.W. Norton & Company. p. 167.

Pallé E., Goode P. R., Montañés-Rodríguez P., Shumko A., Gonzalez-Merino B., Lombilla C. Martinez, Jimenez-Ibarra F., Shumko S., Sanroma E., Hulist A., Miles-Paez P., Murgas F., Nowak G., Koonin S. E., Earth's albedo variations 1998-2014 as measured from ground-based earthshine observations, Geophysical Research Letters, Volume 43, Issue 9, pp. 4531-4538, 2016.

Pagel B.E.J., Nucleosynthesis and Chemical Evolution of Galaxies, Cambridge University Press, 1997.

Peacock J. A., Cosmological Physics, Cambridge University Press, 1999.

Piovan L., Chiosi C., Merlin E.,Grassi T., Tantalo R., Buonomo U. and Cassará L.P., Formation and Evolution of the Dust in Galaxies. I.II.III, astro-ph.GA, 22 Jul 2011.

Portinari L. & Chiosi C., On star formation and chemical evolution in the Galactic disc, A&A, 350, 827, 1999.

Prantzos N. & Aubert O., On the chemical evolution of the galactic disk, A&A, N. 302, 69, 1995.

Prantzos N. & Silk J., Star Formation and Chemical Evolution in the Milky Way: Cosmological Implications, ApJ, N. 507, 229-240, 1998.

Prantzos N. & Boissier S., Metallicity in damped Lyman-a system: evolution or bias?, MNRAS, N. 315, 82-88, 1999.

Prantzos N., On the Galactic Habitable Zone, Dec 2006, https://arxiv.org/abs/astro-ph/0612316

Prantzos N., On the Galactic Habitable Zone, Space Science Reviews, N. 135, 313-322, 2008.

Ramirez R.M. & Kaltenegger L., A Volcanic Hydrogen Habitable Zone, ApJL, 837:L4, 2017.

Ramirez R.M. & Kaltenegger L., A Methane Extension to the Classical Habitable Zone, ApJ, 858, 72, 2018.

Ramirez R.M., A More Comprehensive Habitable Zone for finding Life on Other Planets, Geosciences, 8, 280, 2018.

Rees, M., I sei numeri dell'universo, Rizzoli, 2002.

Reeves H., La crescita della complessitá in un universo in espansione, (pg. 61 in: Il principio Antropico, a cura di Giacomini B.) Ed. Spazio Libri Editori, 1991.

Roškar R., Debattista V.P., Quinn T.R., Stinson G.S. and Wadsley J., Riding the Spiral Waves: Implications of Stellar Migration for the Properties of Galactic Disks,684, L79-L82, 2008 (a).

Roškar R., Debattista V.P., Stinson G.S., Quinn T.R., Kaufmann T., and Wadsley J., Beyond Inside-Out Growth: Formation and Evolution of Disk Outskirts, 675, L65-L68, 2008 (b).

Schwarzschild M., Structure and evolution of the stars, Princeton University Press, Dover, 1958.

Secco L., in "Questions of Modern Cosmology: Galileo's Legacy", by D'Onofrio, Mauro; Burigana, Carlo, ISBN 978-3-642-00791-0. Berlin: Springer-Verlag Heidelberg, 391-399, 2009.

Simpson G.G., I fossili e la storia della vita, from the original: Fossils and the History of Life, Zanichelli Editore, 1986.

Spano M., Marcelin M, Amram P., Carignan C., Epinat B. & Hernandez O., GHASP: an H kinematic survey of spiral and irregular galaxies- V. Dark matter distribution in 36 nearby spiral galaxies, MNRAS, N. 383, 297-316, 2008.

Tomasella L., Tesi di Laurea Specialistica: Evoluzione dell'obliquitá della Terra e Marte, Relatore: Vanzani V, Correlatore: Marzari F., Dipartimento di Fisica di Padova, 1992.

Tomasella L., Marzari F. & Vanzani V., Evolution of the Earth obliquity after the tidal expansion of the Moon orbit, Planetary & Space Science, 44, 427, 1996.

Tremaine, S. 1993, Planets Around Pulsars, ASP Conference Series, 36, 335. Vol 44, N. 5, 427-430, 1995.

Urey H.C., The Planets: Their Origin and Development, Yale Univ. Press, New Haven, 1952.

Veras, D., & Evans, N.W.,Exoplanets beyond the Solar neighbourhood: Galactic tidal perturbations, MNRAS, 430, 403, 2013.

Wallace, J.M., Hobbs, P.V., Atmospheric Science, Second Edition, Elsevier, pg.10,2006.

Ward W. R., Large-scale variation in the obliquity of Mars, Le Scienze, N. 181, 260-262, 1974.

Zhang S. & O'Neil C., The early geodynamic evolution of Mars-type planets, 265, 187, 2016.

Zsom A., Seager S., de Wit J., Stamenković V., Toward the Minimum Inner Edge Distance of the Habitable Zone, ApJ, 778, 109, 2013.